AIAA 2003-0745

AWS Figure of Merit (FOM) Developed Parameters from Static, Transonic Model Tests

J. E. Lamar, F.J. Capone and R. M. Hall
NASA Langley Research Center
Hampton, Virginia

41st AIAA Aerospace Sciences Meeting and Exhibit

6-9 January 2003
Reno, Nevada

AWS FIGURE OF MERIT (FOM) DEVELOPED PARAMETERS FROM STATIC TRANSONIC, MODEL TESTS

by

John E. Lamar*, Francis J. Capone† and Robert M. Hall*
NASA Langley Research Center
Hampton, VA 23681

ABSTRACT

This paper provides an approach to answer the question of whether one can rely solely on static data taken during a transonic model test to provide the certainty needed that a new aircraft will or will not have Abrupt Wing Stall (AWS) events during its flight operations. By comparing traditional- and alternate-static-Figures of Merit (FOMs) with the Free-To-Roll (FTR) response data, a rational basis for assessing the merits of using standard testing techniques for the prediction of AWS events has been established. Using the FTR response data as a standard, since these results compare well with flight, the conclusion from this study is that neither traditional nor alternate FOMs can be trusted to provide an indication as to whether a configuration will or will not have AWS tendencies. Even though these FOMs may flag features which have a high degree of correlation with the FTR response data, there are as many or more of these FOM flagged features which do not correlate. Thus, one needs to use the FTR rig to assess AWS tendencies on new configurations.

* Aerospace Engineer, Configuration Aerodynamics Branch, Associate Fellow, AIAA

† Aerospace Engineer, Configuration Aerodynamics Branch

NOMENCLATURE

Ail	Aileron deflection angle, positive down
AFOM	Alternate FOM
AWS	Abrupt Wing Stall
A1, A2, A3	Coefficients in ΣFOM,3
C_L	Lift coefficient
$C_{L\alpha}$	Lift curve slope
C_l	Rolling moment coefficient
$C_{l,rms}$	root mean square of the C_l
$C_{l\beta}$	Dihedral effect
C_N	Normal force coefficient
$C_{N,rms}$	root mean square of the C_N
C_{WRBM}	Wing root-bending moment coefficient
$C_{WRBM,rms}$	root mean square of the C_{WRBM}
FCL	Flight Control Law, used with the F/A-18E/F aircraft
FOM	Figure Of Merit
FTR	Free-To-Roll
ISE	Inboard Snag Extension along the leading edge
LE, LEF	Leading edge flap deflection angle, positive down
LERX	Leading Edge Root Extension for AV-8B
LEX	Leading Edge Extension for F/A-18E
M	Mach number
N/A	Not Available
rms	root mean square
Rn	Reynolds number, given in terms of millions per foot

16FTT	16 Foot Transonic Tunnel at NASA Langley; officially known as 16-ft TT
TE, TEF	Trailing edge flap deflection angle, positive down
TFOM	Traditional FOM
α	angle of attack, degrees
β	angle of sideslip, degrees
ΔC_l	change in rolling moment coefficient, $C_{l\|\alpha}$ - $C_{l\|\alpha=0^\circ}$
θ	pitch-strut angle, degrees
ΠFOM	Product FOM form
ΣFOM,3	A summation FOM form
ϕ	model roll angle, degrees

Subscripts

R or L	for right or left wing, respectively

INTRODUCTION

Naturally occurring flight asymmetries on starboard and port wings – associated with small but fixed geometrical differences, control-surface-deflection differences about the centerline, or onset flow differences – normally do not give rise to significant, unplanned rolling motions with just a small change in angle of attack. Instead, these asymmetries are resisted by particular aircraft aerodynamic stability derivatives, primarily dihedral effect and damping-in-roll. However, for some aircraft and flight-condition combinations, the asymmetries are large and develop from an abrupt stall on one wing. This Abrupt Wing Stall (AWS) can lead to rolling moments and, consequently, wing-drop, wing-rock or other undesirable lateral stability phenomenon[1] during high-subsonic or transonic maneuvers – typically a wind-up-turn.

The preceding AWS events can also be described in two other ways; firstly, as an asymmetric airflow across the wings which produces an unanticipated rolling moment resulting in a lateral dynamic response of the aircraft. Moreover, the abruptness of the stall event on one wing during these maneuvers occurs with no apparent change in lateral stick. Secondly, as "…an uncommanded motion seen by the pilot as a divergence in roll and incipient departure. Typically the roll rates are not high, being of the order of 10^o-20^o/sec. It is clearly beyond both the aiming limit and the tactical maneuvering limit, and immediate recovery action is required in order to maintain full control."[2,3] Many production aircraft, mostly fighters, have had an asymmetrical-lift problem in which separated flow develops on one wing but remains attached on the other[1].

The latest USA fighter airplane to have such phenomenon is the pre-production version of the F/A-18E/F aircraft with wing-drop at transonic speeds. Another airplane still in the inventory that also has developed AWS is the AV-8B at the extremes of its operating envelope. These facts led the AWS program wind-tunnel test team to develop a plan for testing four models — the preceding two plus the F/A-18C and the F-16C — in the Langley 16FTT at $M < 1$. The latter two were chosen because these aircraft do not demonstrate AWS events in flight. Hence, one goal of this testing was to look for differences in the model static measurements, or Figures Of Merit (FOMs), that would provide insight or an indication of why these two groups of aircraft have different, lateral flight-characteristics.

Correlations are sought between the various potential FOMs and Free-To-Roll (FTR)[4] or available flight response data in order to assess reliability of the proposed FOMs. A

part of this study is to establish whether there is at least one FOM that is a necessary and sufficient condition for AWS events. If the answer to this is no, then is there one FOM which is at least a necessary condition for AWS.

In order to accomplish the preceding, this paper documents various potential FOMs from static wind-tunnel tests, examines the extent to which they have proven useful in the prediction of AWS events at high-subsonic and transonic speeds for these four aircraft models by comparing with the FTR response data, and considers other FOMs which can be developed from static data. Both traditional and alternative FOMs are defined and considered in this study across the α, Mach and flap-setting range tested.

Data are reported in this paper for each combination of flap-set and Mach number for the four configurations tested without regard to whether the flaps are on schedule. Even though the aircraft flap-schedules were available to the authors for these models, such knowledge will not be known to an aerodynamicist for a new airplane model prior to test; hence, this reporting can be considered as a "blind test". Because of the preceding, the data collected on many of the tested flap-set and Mach number combinations are for conditions the studied aircraft will never fly.

In order to obtain approval for releasing this paper to the public, quantitative information has been removed from most vertical scales as per guidelines from the Department of Defense.

TRADTIONAL FOM STUDIES

Background

The traditional FOMs (TFOMs) from static wind-tunnel tests include the lift curve break, denoted by either the C_L vs. α curve or the $C_{L\alpha}$ slope change, and the C_l, $C_{l,rms}$, C_{WRBM}, and $C_{WRBM,rms}$ curves vs. α. Experience has taught that changes in these parameters can be indicative of changes in the flow topology which can lead to the kinds of aircraft response denoted as AWS flight events. A discussion of each parameter group follows.

C_L vs. α or $C_{L\alpha}$ slope change

Unlike a transport aircraft wing that has basically a linear lift curve followed by a break in the curve near $C_{L,max}$, a fighter aircraft may have multiple breaks in its lift curve associated with the redistribution of lift between the main wing and the LEX. At low values of α the flow on the main wing is attached and the LEX produces very little vortical flow or lift due to the small incidence angle. However, with increasing α the main wing outer panel begins to stall and the LEX vortex begins to develop more lift over itself as well as over that part of the wing behind it. The redistribution of lift at transonic speeds is further complicated by unsteady flow[5,6] produced by the varying amounts of separation, especially shock-induced, associated with Mach number- and flap-changes.

Any discontinuities in the slope of the lift (normal-force) curve reflect changes in the flow physics and may be indicative of a problem area–buffet onset, wing drop, wing rock, or loss of roll-damping. This is supported by Reference 7, that claimed the lift curve "should not have any

nonlinearities," and Reference 8, which questioned whether lift beyond the kink "is usable" for nonlinear curves, respectively. Hence, the manner in which the actual flow transitions from the two flow topologies of predominately wing attached-flow to predominately wing-outer-panel-separated-and-LEX-vortex is critical as to whether wing drop or AWS may be expected to occur.

The sketches in Figure 1 (a) show the kinds of C_L vs. α or $C_{L\alpha}$ slope changes typical of an AWS event.

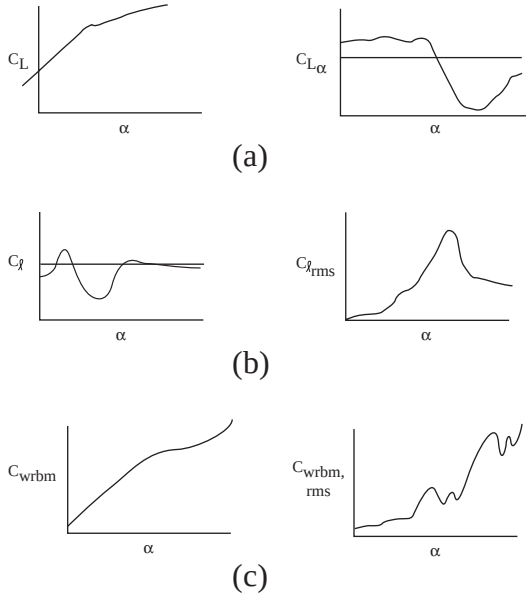

Figure 1. Notional graphs of static aerodynamic coefficients which could indicate AWS events.

C_l and $C_{l,rms}$

The rationale for considering asymmetries in rolling moment is that uncommanded lateral motions are the result in flight of one wing stalling before the other. Thus this stall feature may be captured in the tunnel by examining rolling moments[9] for nominally $\beta = 0^o$. The moments may produce either positive or negative values depending on which wing stalls. (A previous test for the pre-production F/A-18E model [16FTT-523] has established that C_l has a transonic Mach number dependency at $\beta = 0^o$.) However, if the model experiences lateral dynamics, then the time-averaged result of rolling moment may be small even through instantaneous values are large. On the other hand, one would expect variance, or rms, of the signal to grow. The sketches in Figure 1 (b) show steady (time-averaged — 50 samples total; 10 samples/sec for 5 seconds) and unsteady (rms) rolling moments that can occur during AWS events. Large amplitude excursions of C_l over a limited α range are associated with a wing-drop event. By contrast, C_l sinusoidal envelope-excursions with time at a fixed α are more indicative of wing-rock. As this paper focuses on static- and not time-dependent-data, the C_l characteristic sought in the measured results will be that associated with wing-drop.

The characteristic shape associated with AWS for the $C_{l,rms}$ is a rapid rise and then a decrease (an envelope-excursion), but the ending level is higher than that at the beginning.

C_{WRBM} and $C_{WRBM,rms}$

The rationale of using wing-root bending moment slope changes is that it produces similar changes to the lift or normal force curves except that it is directly measuring a rolling moment at the location of the gauge. In other words, it is measuring not only a sense of the lift increase or loss, but also whether this increase or loss is inboard or outboard.

Sketches in Figure 1 (c) show typical steady and unsteady (rms), wing root-bending moments. From previous studies done with these parameters, the conclusions were: (1)

wing bending more readily illustrates breaks in the lift, or normal force, than does the six component balance information for lift or normal force; (2) breaks in the wing bending moment curve – positive or negative – appear to be a potential FOM although how much break does it take to trigger wing drop remains to be determined; and (3) onset of the rms excursion (as seen by an envelope) in wing root bending moment is another good correlator with trends seen in both other tunnel parameters and flight.

Background Summary

Sudden or rapid variations in the preceding curves with α are due to flow topology changes occurring on one or both wings. These changes include flow transitions from the predominately wing-attached-flow to predominately shock-induced-separated, unsteady, wing-outer-panel and a LEX-vortex. The data curves are also affected by flow conditions for which the flow separates from the lower-surface of an over-deflected leading-edge flap. A correlation of the impact of these flow changes, as measured by static data and evaluated via the response of the FTR rig, follows.

Approach

There are two main elements in the approach to compare the FTR response data with static-wind-tunnel results. The first is that the FTR data is considered to be the standard, as it compares favorably with flight.[10,11] Moreover, it is considered here to be a reliable indicator of AWS flight events for $\alpha \geq 6^{o}$. The FTR-FOM parameter[10,11] for AWS events yielded the following results:

-For no significant activity, denoted as a green box;
-For moderate activity, denoted as a yellow box; and
-For severe activity, denoted as a red box.
A partial sample follows.

FTR-FOM					
θ, degrees	11.5	12.0	12.5	13.0	14.0

Figure 2. Sample FTR-FOM results with pitch-strut angle. $\theta \approx \alpha$.

There are two consequences of this table. They are:

a. Noticeable FTR activity, or an AWS event, occurs at the α for which there is an associated red or yellow filled cell.
b. AWS events may happen at a single value of α or cover an α range.

The second element deals with agreement between the data-sets. Agreement is called between a static parameter and an AWS event if the α associated with any portion of the parameter break (for C_L, $C_{L\alpha,}$ and $C_{WRBM,}$) or an excursion-envelope (for C_l, $C_{l,rms}$, and $C_{WRBM,rms}$) occurs within 1^{o} of the α for an event. (A static-data feature, i.e., break or envelope excursion which is historically characteristic of an AWS event in that TFOM, is called a flag in this paper.)

Static & FTR data comparisons

This section presents basic graphical comparison plots of the static and FTR response data. Response data are denoted by arrows, which have been color-coded according to Figure 2, and are plotted at the values of α for which AWS events occur. No green arrows are plotted as we seek to highlight the correlations with AWS events, not non-events.

Before undertaking the data-set comparisons, there was a tendency to discount many small slope changes or data excursions as being within the measurement accuracy. However, after observing that

many arrow sets occurred in these same α regions, slope changes (parameter break) of any significance were counted. (Unfortunately, it is not possible to establish a direct correlation between an AWS event and a quantifiable threshold for a TFOM change which is generally applicable.) The preceding is of importance because the vertical scales on the TFOM graphs are the same for all four configurations and were not adjusted for each configuration, parameter, flap-set or Mach number. Finally, the authors have made an attempt to apply the guidance provided in the **Background** section in performing these comparisons; however, even with the best intentions this process has been conducted subjectively and has an estimated flagged-feature-count-accuracy of ±1 per curve. A large part of the subjectivity is directly related to determining how much of a TFOM change is enough for a feature to be flagged and counted.

Examples and Scoring

In order to acquaint the reader with the technique employed for assessing agreement between the two data types, an example of each basic plot and an explanation of how the agreement was scored is given for each curve. Scores for all TFOM parameters are summarized in subsequent tables.

Application of TFOM Criterion

The criterion for agreement between the static and the FTR response data has been given in the **Approach** section. This is applied to the data and reported in the following manner as a score: the denominator is the sum of red and yellow arrows; the numerator is the number of matches between the two data sets – FTR events and static-data flagged features of breaks in curves or envelope excursions – for each TFOM; and the parenthetical number denotes the count of flags for which there was no FTR-FOM arrow within 1° of α. The latter are called misses. Figures 3 to 5 shows red and/or yellow arrows associated with each curve. Note that the arrow outline is **solid** or **dashed** signifying the curve to which it belongs. (In subsequent figures there may be an additional curve and arrow-outline which is **long-and-short-dashed**.)

C_L vs. α or $C_{L\alpha}$ slope change

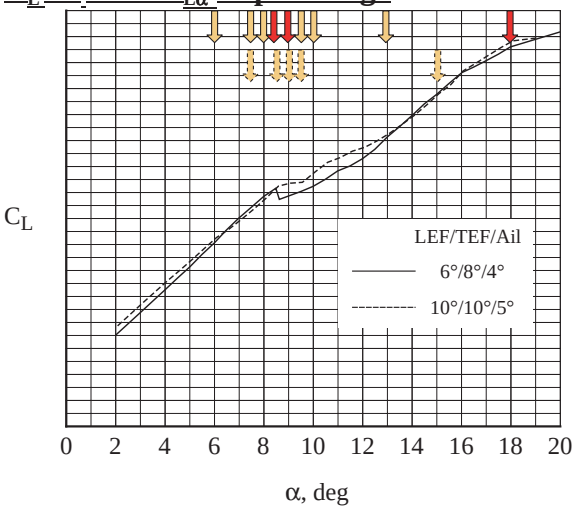

Figure 3. Pre-production F/A-18E at M = 0.9. (a) Lift curve.

The C_L TFOM in Figure 3 (a) shows the **solid curve** to have sharp, or rapid, slope changes at values of α of 6°, 8.5°, 10.5°, 12.5°, 13°, 16° and 18°. All nine arrows fall within 1° of a slope change, so we have agreement or a score of 9 out of 9. However, at α = 16° there is a slope change (flag) with no corresponding event or arrow. Hence, the score for this curve is 9(1)/9. The **dashed curve** has changes at values of α of 8.5°, 9.5°, 10.5°, 13°, 16° and 18°, which produces agreement with five events or arrows and two misses (values of α of 13° and 18°) for a score of 5(2)/5.

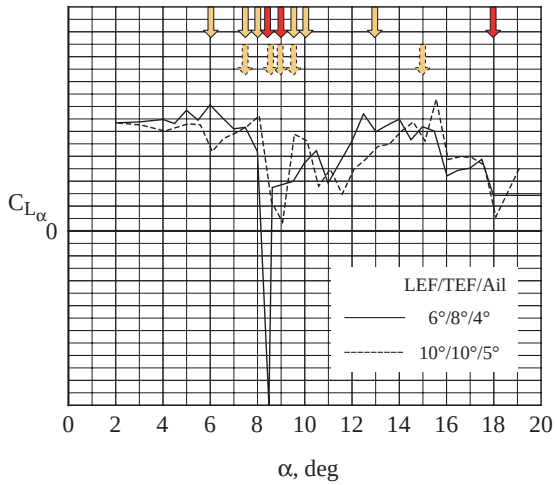

Figure 3. (b) Lift curve slope.

The $C_{L\alpha}$ TFOM in Figure 3(b) shows the **solid curve** to have multiple changes, some large and others not so big. They occur at values of α of 6°, 8°, 8.5°, 9°, 9.5°, 11°, 12.5°, 13°, 15.5°, 16°, 17.5° and 18°. All nine arrows have agreement but there are two misses (values of α of 15.5° and 16°), so the score for this curve is 9(2)/9. The **dashed curve** has changes at values of α of 6°, 8°, 9°, 9.5°, 10.5°, 11°, 11.5°, 15.5°, 16°, 17.5° and 18°. All five arrows have agreement but there are five misses (values of α of 6°, 11°, 11.5°, 17.5° and 18°), yielding a score of 5(5)/5.

C_l and $C_{l,rms}$

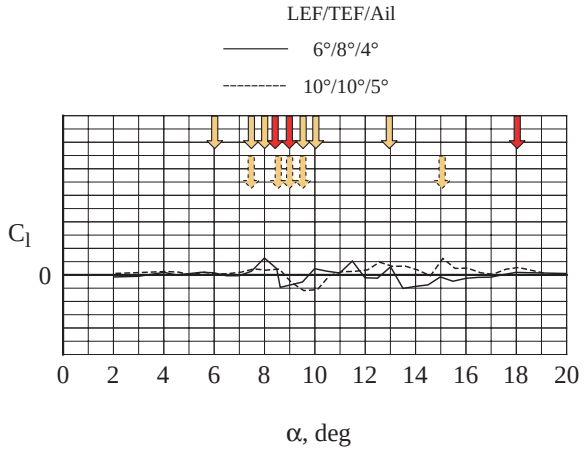

Figure 4. Pre-production F/A-18E at M = 0.9. (a) C_l vs. α.

The C_l TFOM in Figure 4 (a) shows the **solid curve** to have AWS characteristics for values of α from 7° to 10.5°, at 11.5° and from 12.5° to 15°. Nine arrows fall within 1° of an event, but two flags (at values of α of 11.5° and 15°) are missed, so the score for this curve is 9(2)/9. The **dashed curve** has changes for values of α from 7.5° to 11° and from 12.5° to 16°, which produces agreement with five arrows and two misses (flags at values of α of 12.5° and 18°) for a score of 5(2)/5.

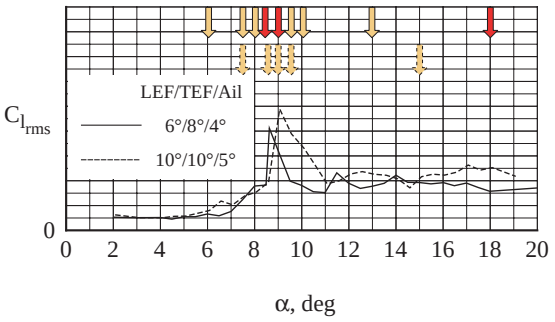

Figure 4. (b) $C_{l,rms}$ vs. α.

The $C_{l,rms}$ TFOM in Figure 4(b) shows the **solid curve** to have AWS characteristics for values of α from 7° to 10°, from 11° to 14° Eight arrows have agreement and no misses, so the score for this curve is 8(0)/9. The **dashed curve** has AWS characteristics from 6° to 11°, from 11.5° to 14.5°, and from 15° to 19°. Five of the arrows have agreement with two misses (flags at values of α of 13° and 17°), yielding a score of 5(2)/5.

C_{WRBM}, and $C_{WRBM,rms}$

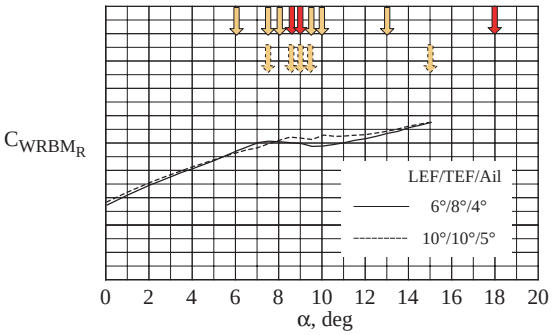

Figure 5. Right Wing-Root-Bending-Moment results for the pre-production F/A-18E at M = 0.9 from 16FTT-523. (Due to test techniques and procedures, the α limit for this test was ≈ 15°.) (a) $C_{WRBM,R}$ vs. α.

The $C_{WRBM,R}$ TFOM in Figure 5 (a) shows the **solid curve** to have AWS characteristics at values of α of 6°, 8° and 10°. Seven arrows fall within 1° of a flag and none are missed, so the score for this curve is 7(0)/9. The **dashed curve** has slope changes at values of α of 7°, 9.5° and 10.5°, which produces agreement with four arrows and no misses for a score of 4(0)/5.

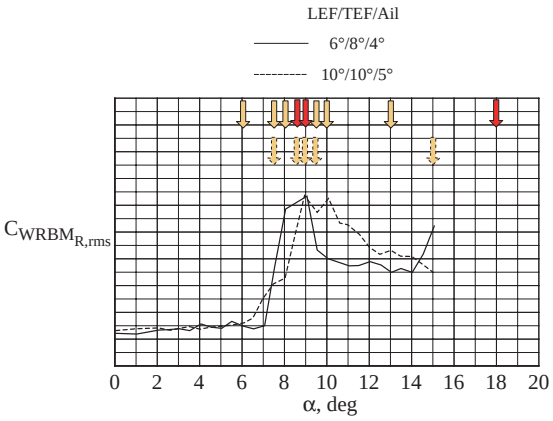

Figure 5. (b) $C_{WRBM,Rrms}$ vs. α.

The $C_{WRBM,Rrms}$ TFOM in Figure 5(b) shows the **solid curve** to have an AWS rapid rise characteristic (envelope) for values of α from 7° to 10.5° and beginning again at 14°. Eight arrows have agreement and with no misses, so the score for this curve is 8(0)/9. The **dashed curve** has AWS characteristics from 6.5° to 12°. Four of the arrows have agreement with no misses, yielding a score of 4(0)/5.

Example Results Summary

There are two general items worth noting from this example set of results. Firstly, the rough equivalency between the number of single or group events/flags measured by both data sets. Secondly, for all these TFOMs there are some values of α for which the static data lead the FTR data, whereas for others the reverse is true. Whether these statements hold true for all four configurations will be assessed after a review of the tables.

Data Comparison Presentations

The graphs are ordered by configuration and decreasing Mach number, with those models associated with AWS events being first. Vertical scales on the graphs remain the same for each TFOM in this section. The test data reported are primarily from the most recent AWS tests, namely 16FTT-563, 564, 565 and 567. There are some previously unreported data used here from 16FTT-523, the initial test of the pre-production F/A-18E model at Langley. In an unpublished study, it was determined that the static data from test 16FTT-565 (the same model tested in the recent sequence) falls within the data repeatability of test 16FTT-523; hence these data sets are used interchangeably.

F/A-18E Pre-production -- 8% Scaled Model Test

	Tunnel-Test	Configuration	Run	M_∞	β, deg	Rn, millions/ft	LEF/TEF/Ail
———	16FTT-565	F/A-18E: Baseline	140.	0.8973	-0.1273	3.817	6°/8°/4°
- - - - - - - - -	16FTT-565	F/A-18E: Baseline	9.	0.8972	-0.1184	3.802	10°/10°/5°

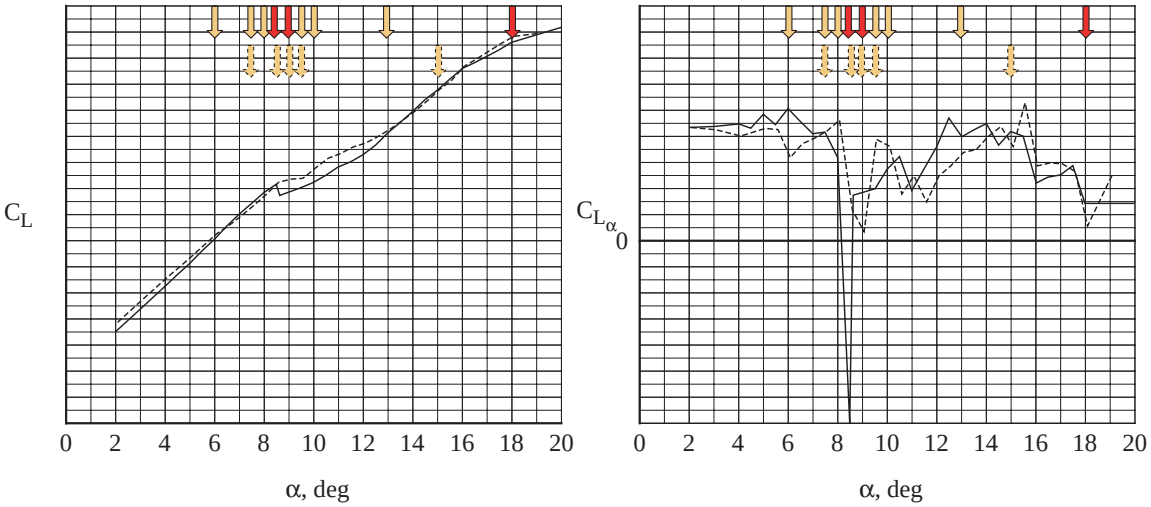

Figure 6. Lift, rolling- and wing-root-bending-moments with FTR data for the F/A-18E pre-production aircraft model at various flap settings and M = 0.9. (a) LEF/TEF/Ail at 6°/8°/4°; and 10°/10°/5°.

	Tunnel-Test	Configuration	Run	M_∞	β, deg	Rn, millions/ft	LEF/TEF/Ail
———	16FTT-565	F/A-18E: Baseline	140.	0.8973	-0.1273	3.817	6°/8°/4°
- - - - - - - - -	16FTT-565	F/A-18E: Baseline	9.	0.8972	-0.1184	3.802	10°/10°/5°

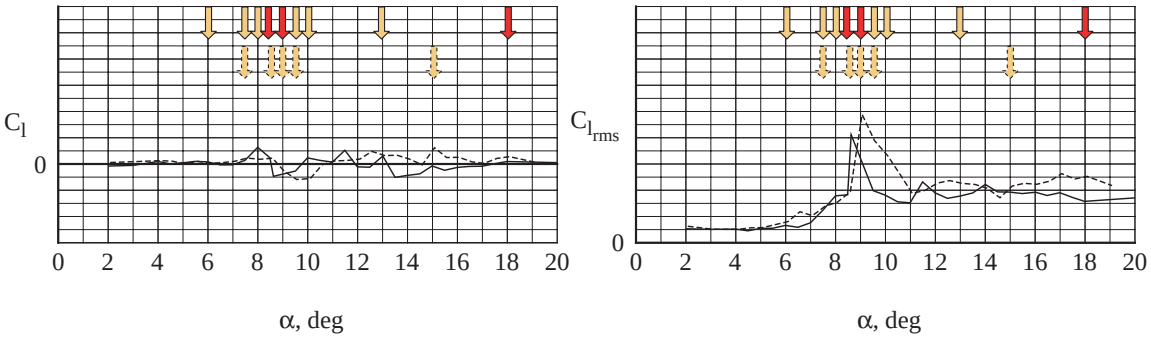

Figure 6. (a) Continued.

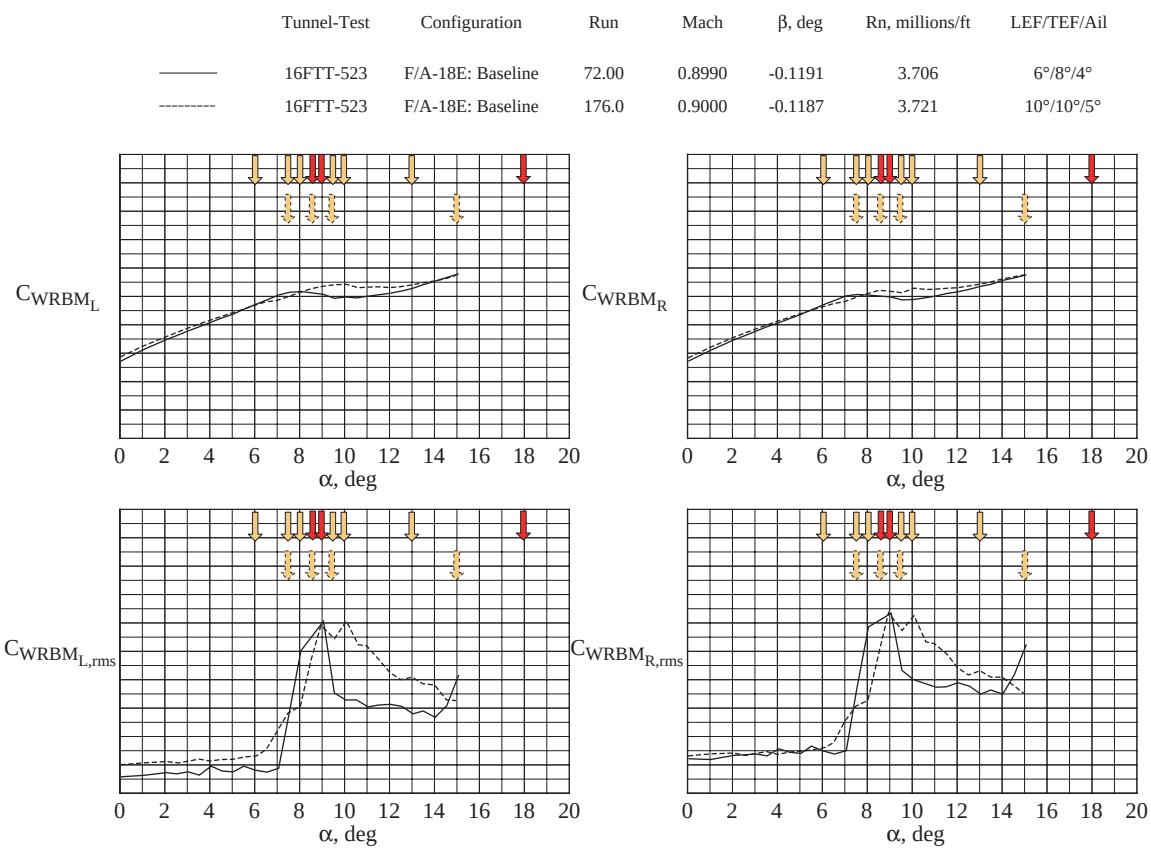

Figure 6. (a) Concluded.

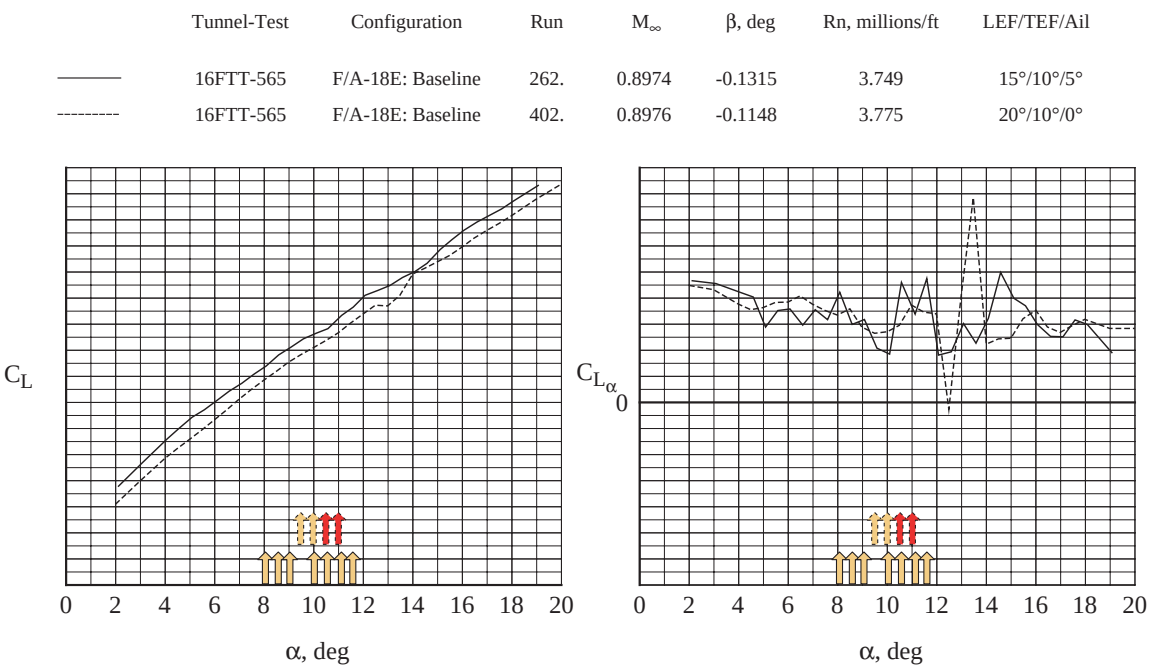

Figure 6. (b) LEF/TEF/Ail at 15º/10º/5º; and 20º/10º/0º.

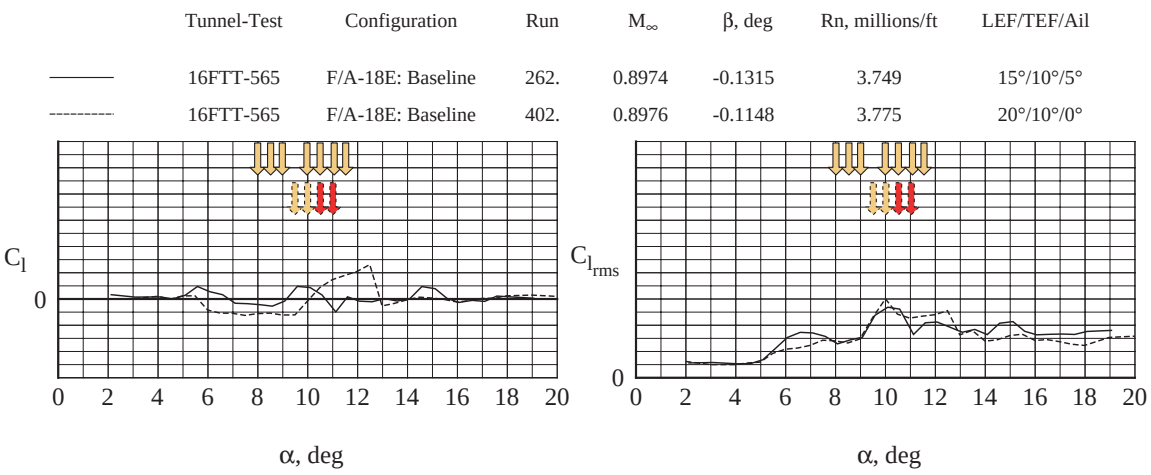

Figure 6. (b) Concluded.

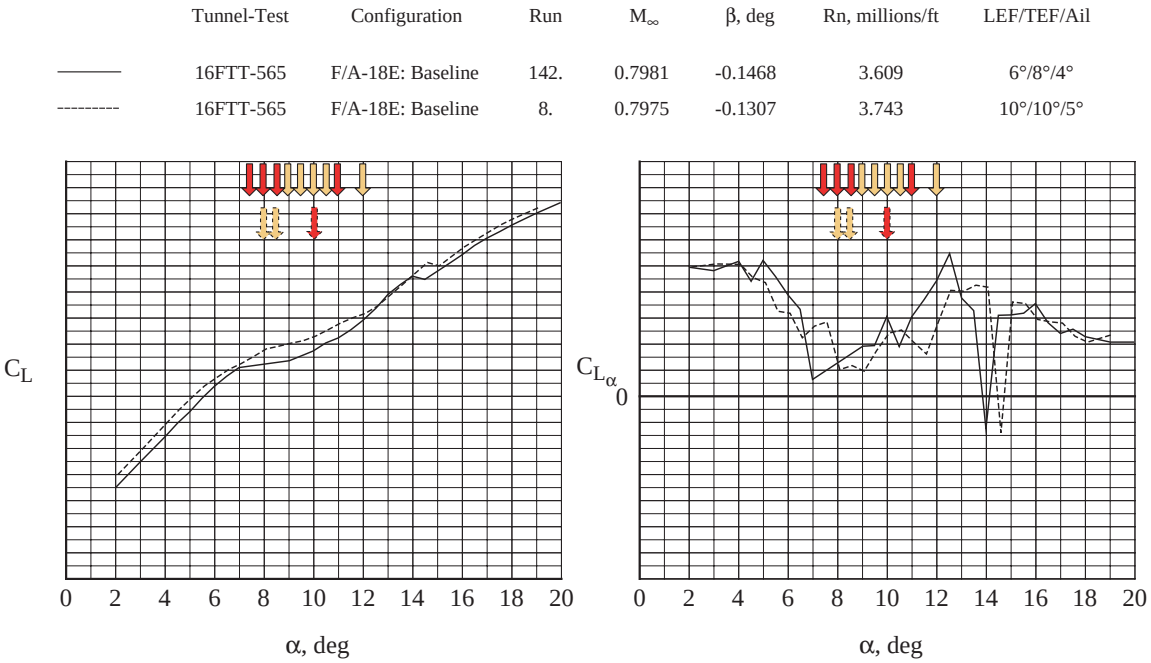

Figure 7. Lift, rolling- and wing-root-bending-moments with FTR data for the F/A-18E pre-production aircraft model at various flap settings and M = 0.8. (a) LEF/TEF/Ail at 6º/8º/4º; and 10º/10º/5º.

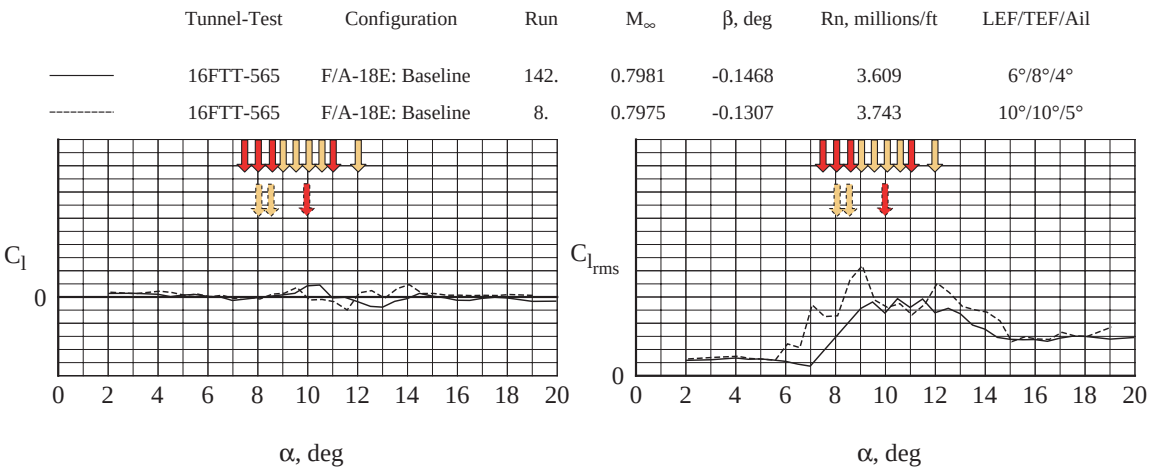

Figure 7. (a) Continued.

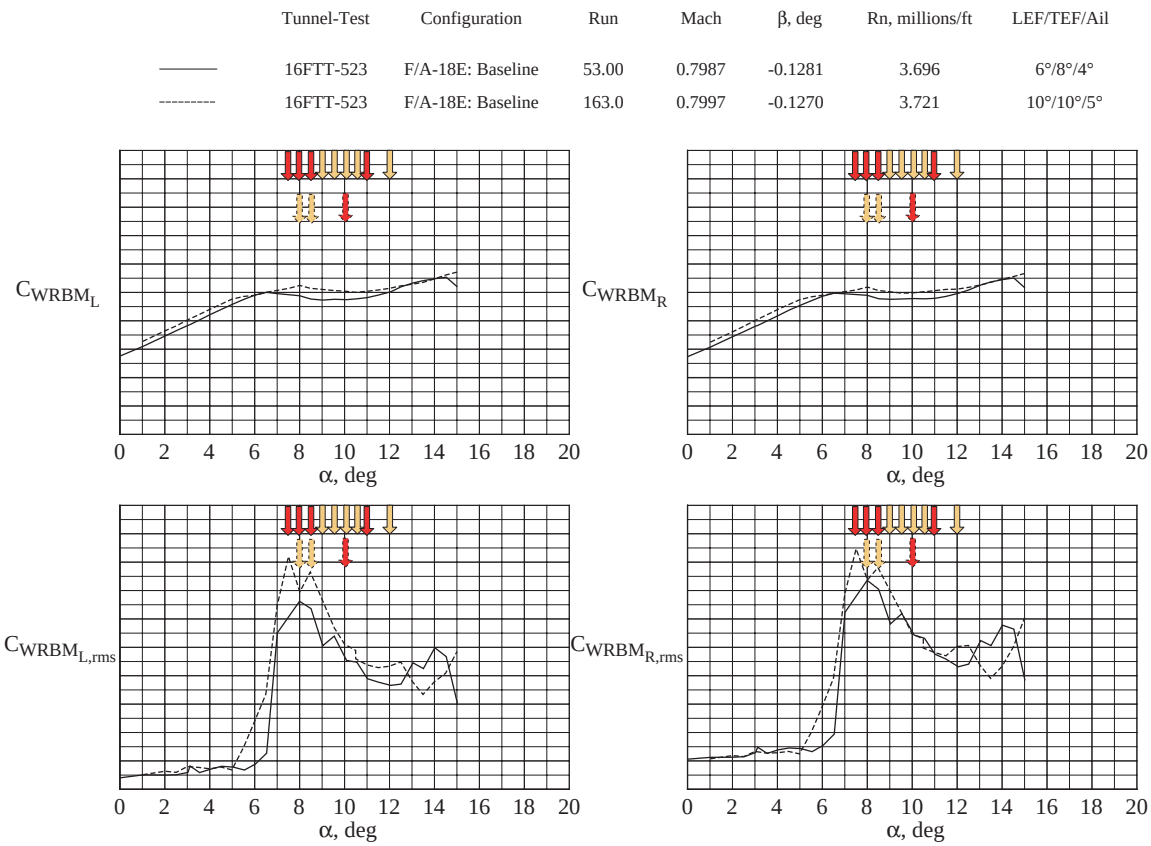

Figure 7. (a) Concluded.

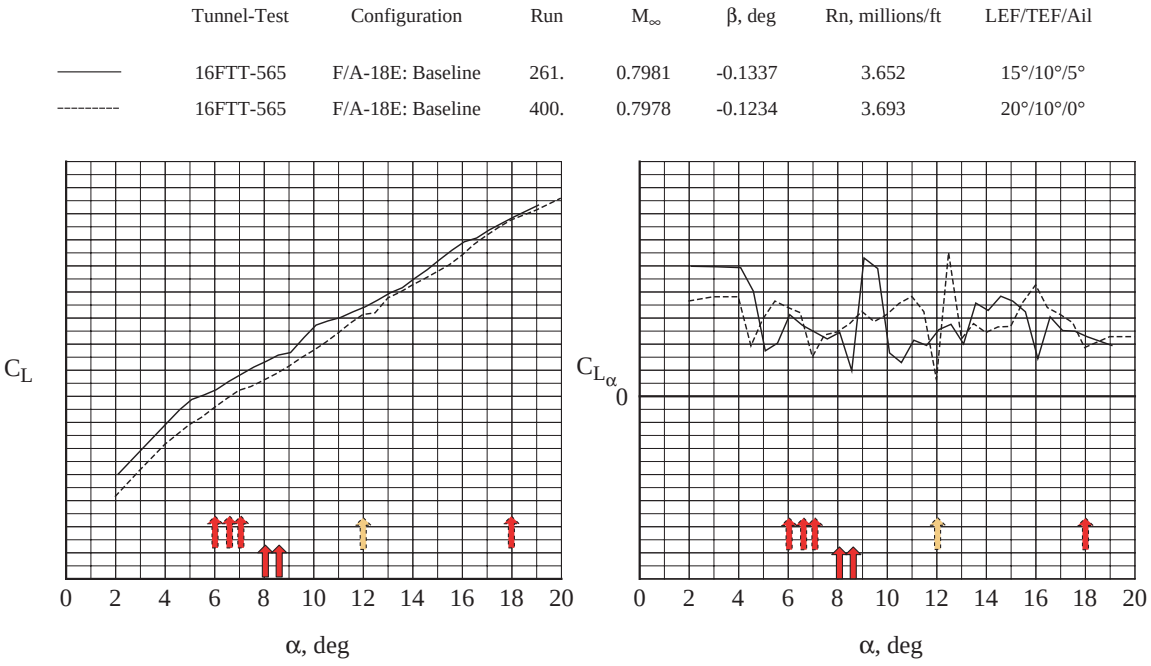

Figure 7. (b) LEF/TEF/Ail at 15°/10°/5°; and 20°/10°/0°.

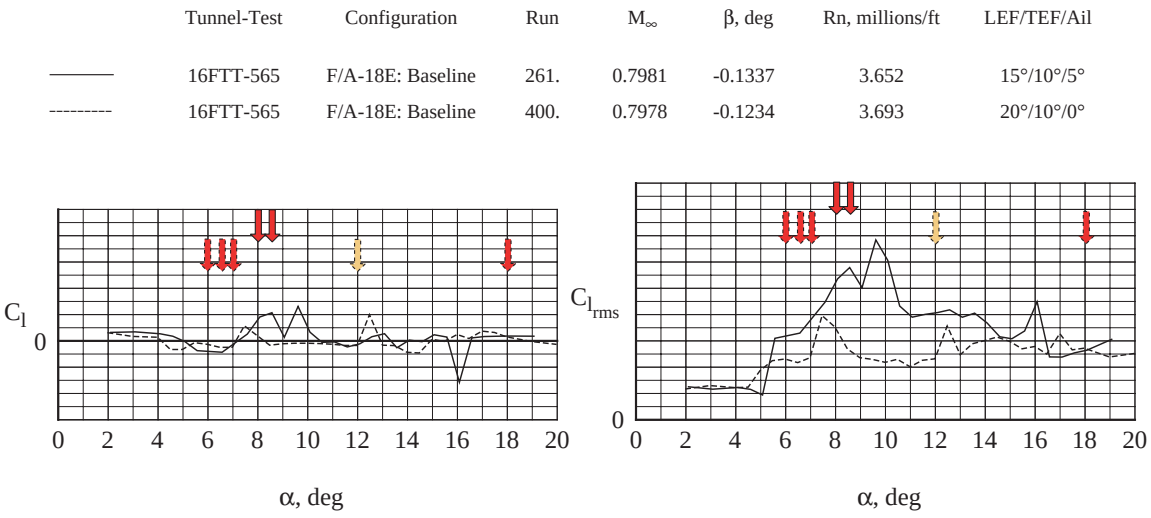

Figure 7. (b) Concluded.

AV-8B -- 15% Scaled Model Test

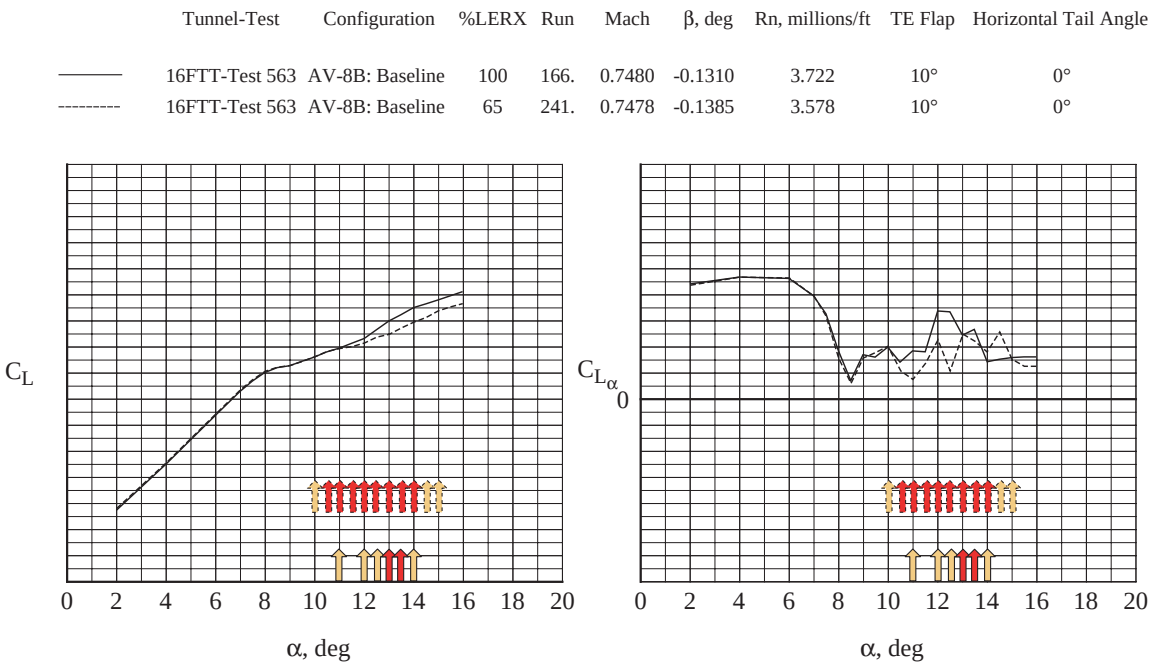

Figure 8. Lift and rolling moments with FTR data for the AV-8B aircraft model at TEF = 10° and M = 0.75. (a) LERX = 100%; 65%.

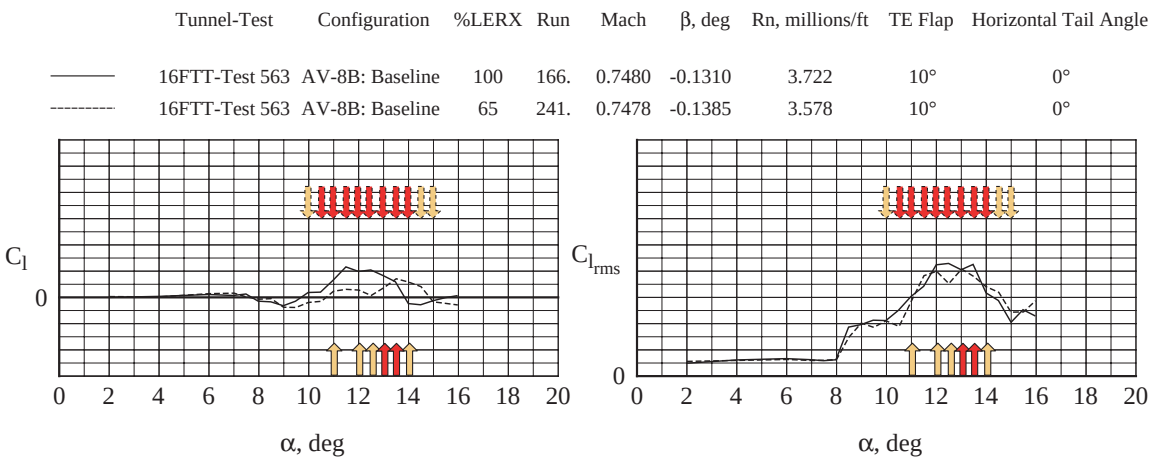

Figure 8. (a) Concluded.

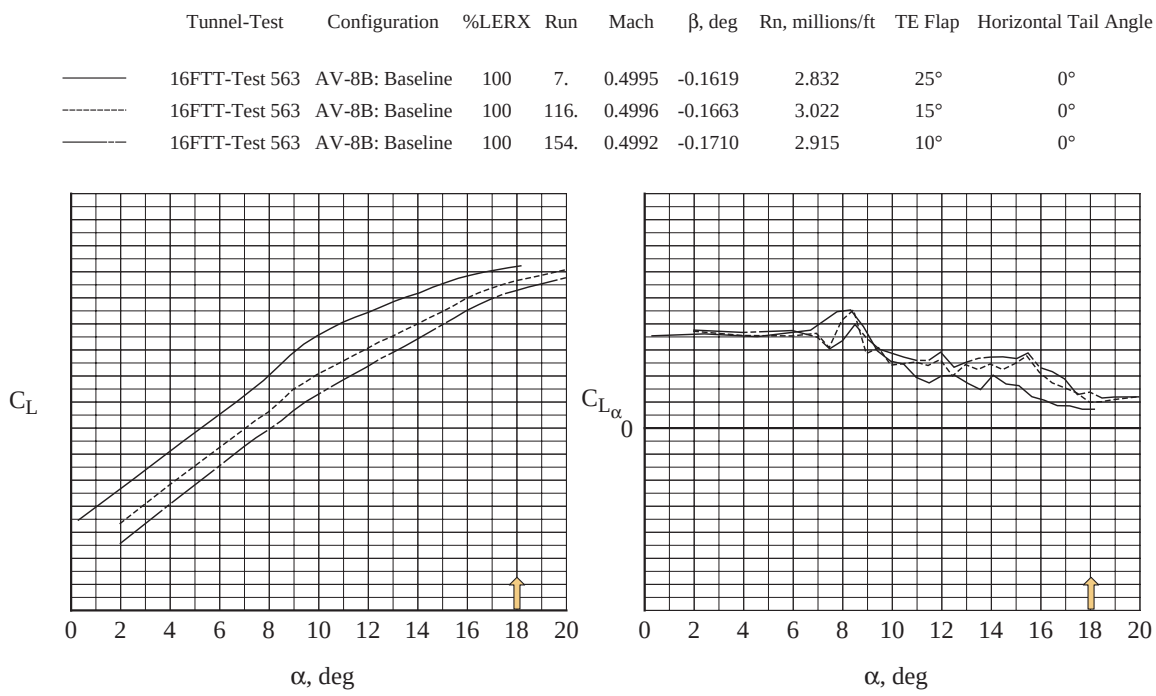

Figure 9. Lift and rolling moments with FTR data for the AV-8B aircraft model at two LERX values and various TEF at M = 0.5. (a) LERX = 100%.

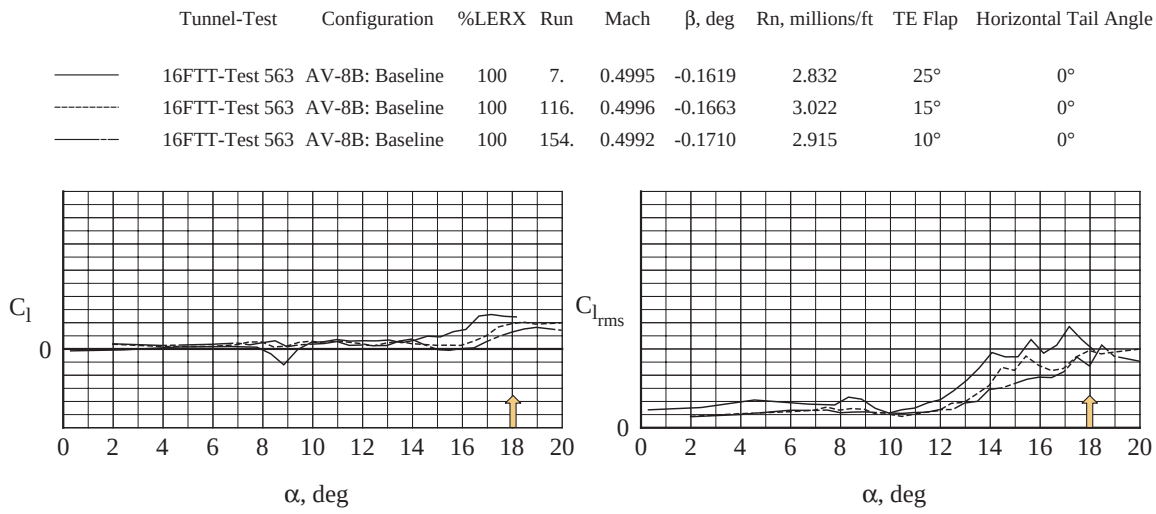

Figure 9. (a) Concluded.

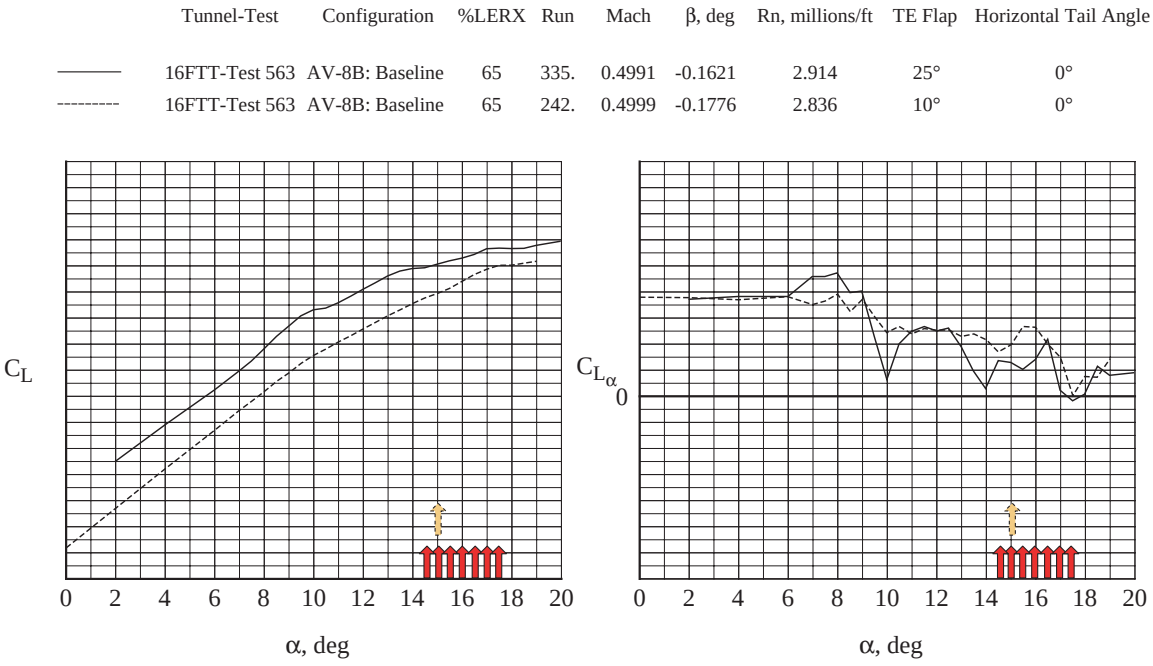

Figure 9. (b) LERX = 65%.

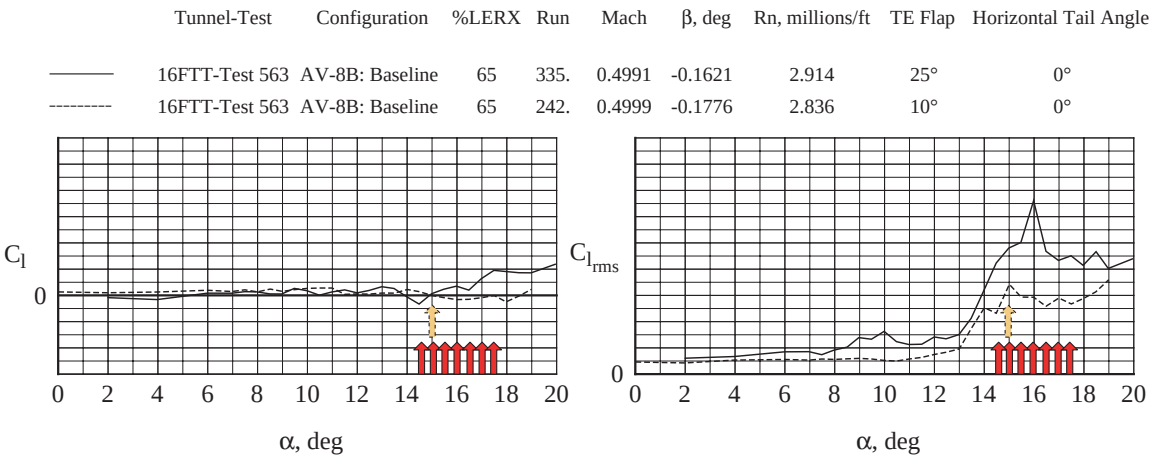

Figure 9. (b) Concluded.

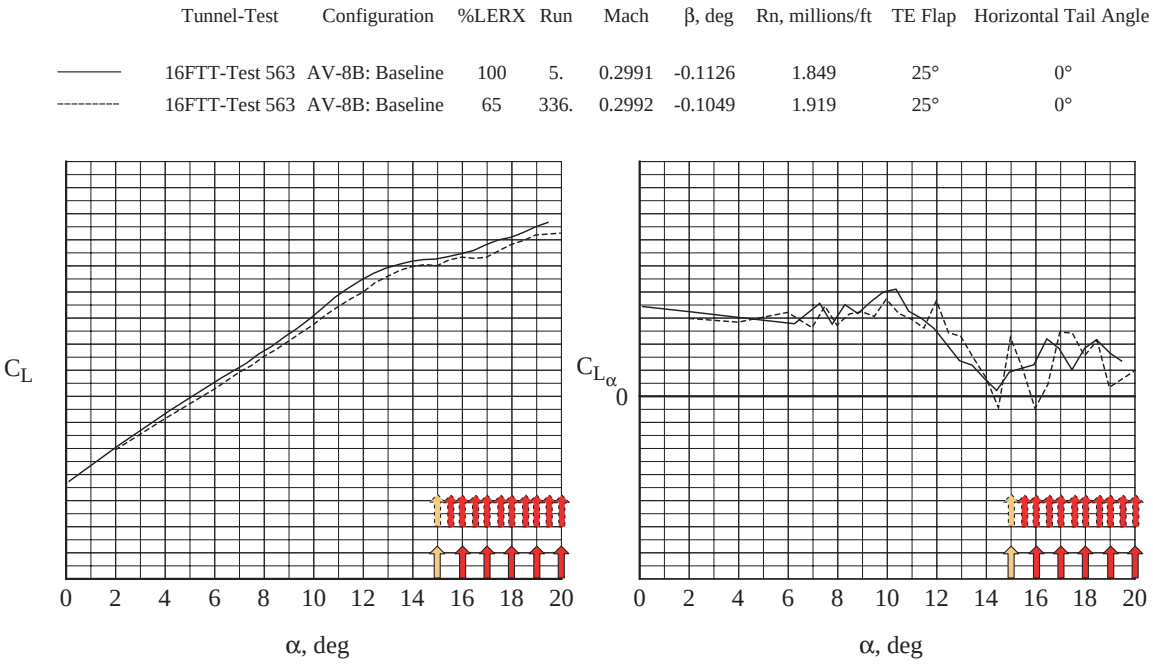

Figure 10. Lift and rolling moments with FTR data for the AV-8B aircraft model at TEF = 25º and M = 0.3. (a) LERX = 100%; 65%.

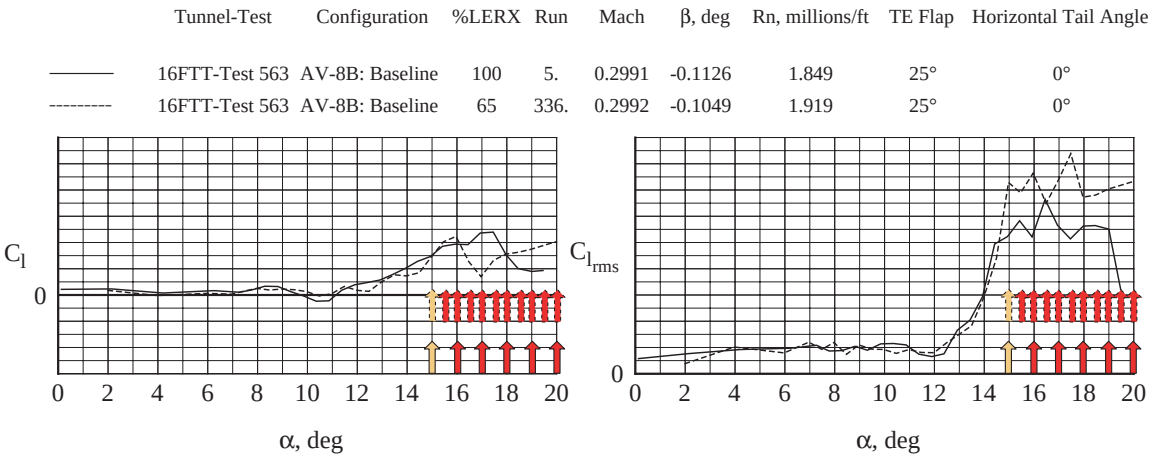

Figure 10. (a) Concluded.

F/A-18C -- 6% Scaled Model Test

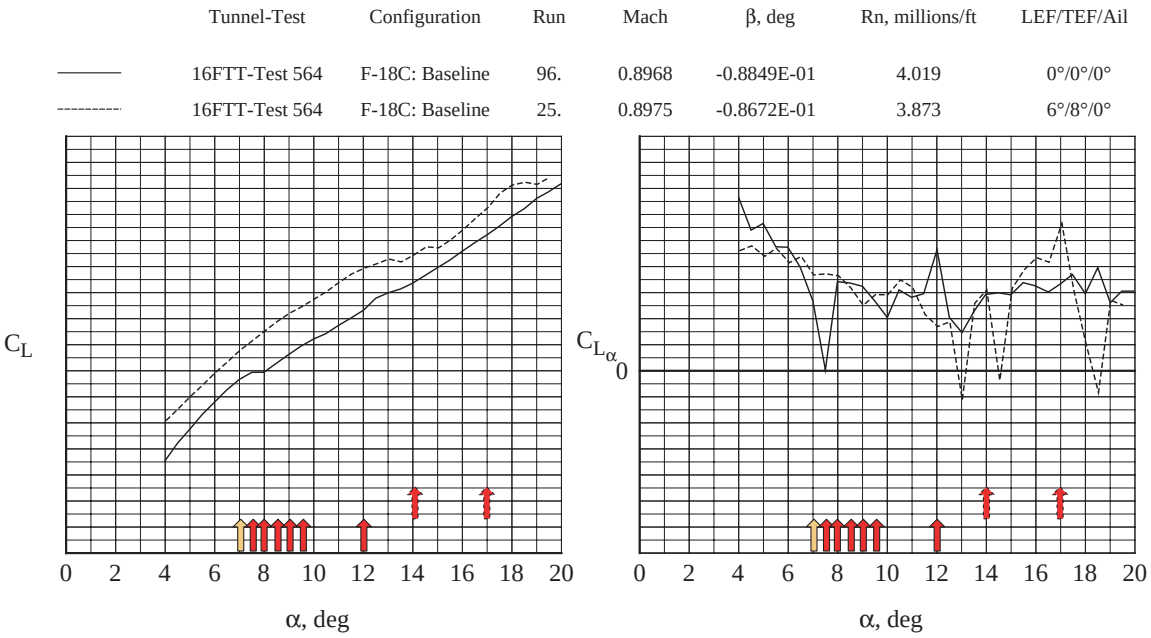

Figure 11. Lift and rolling moments with FTR data for the F/A-18C aircraft model at various flap settings and M = 0.9. (a) LEF/TEF/Ail at 0º/0º/0º and 6º/8º/0º.

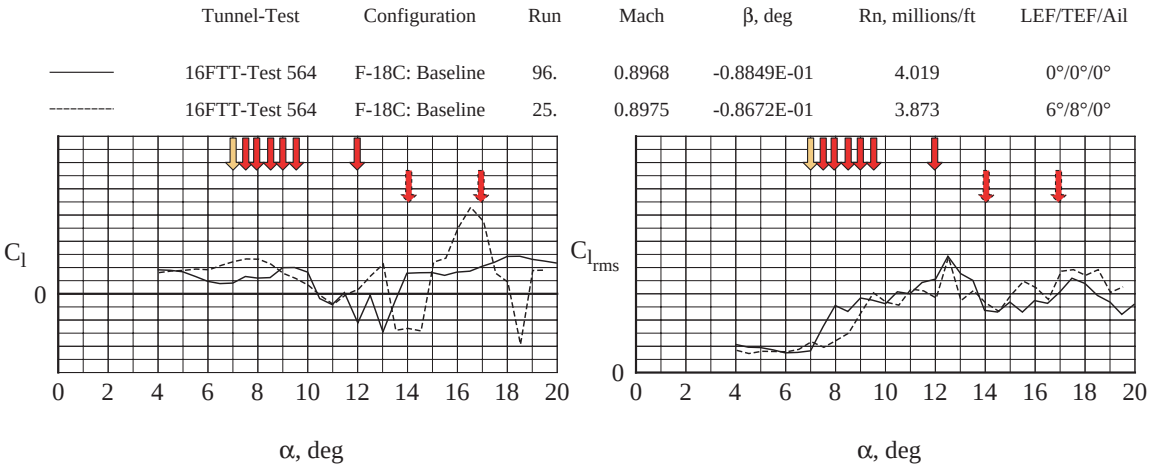

Figure 11. (a) Concluded.

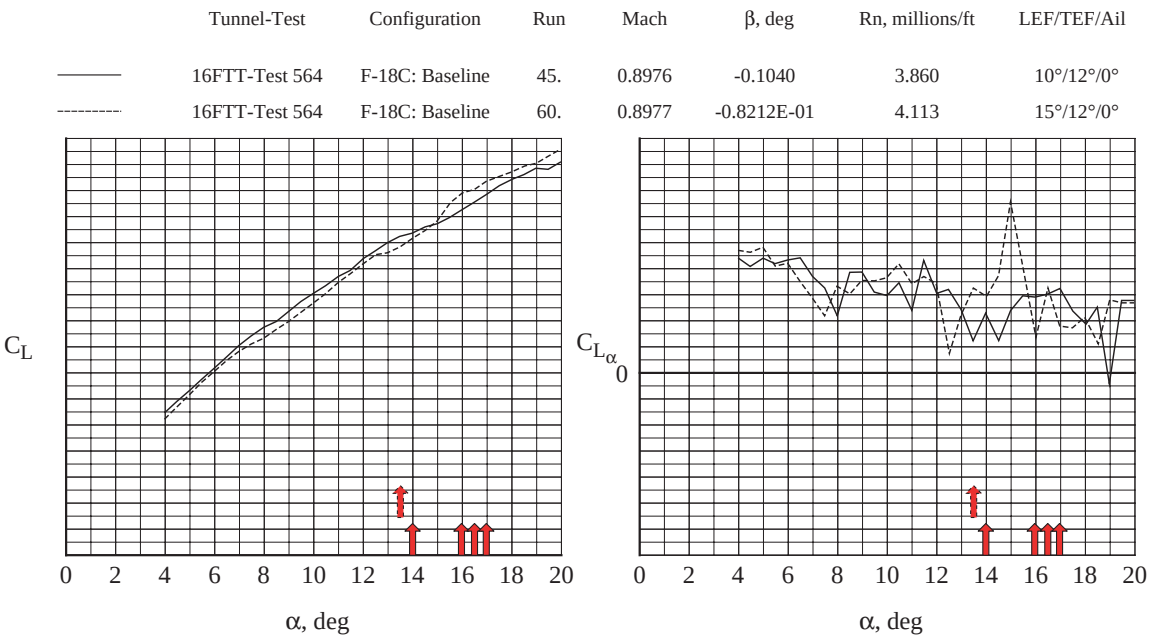

Figure 11. (b) LEF/TEF/Ail at 10°/12°/0° and 15°/12°/0°.

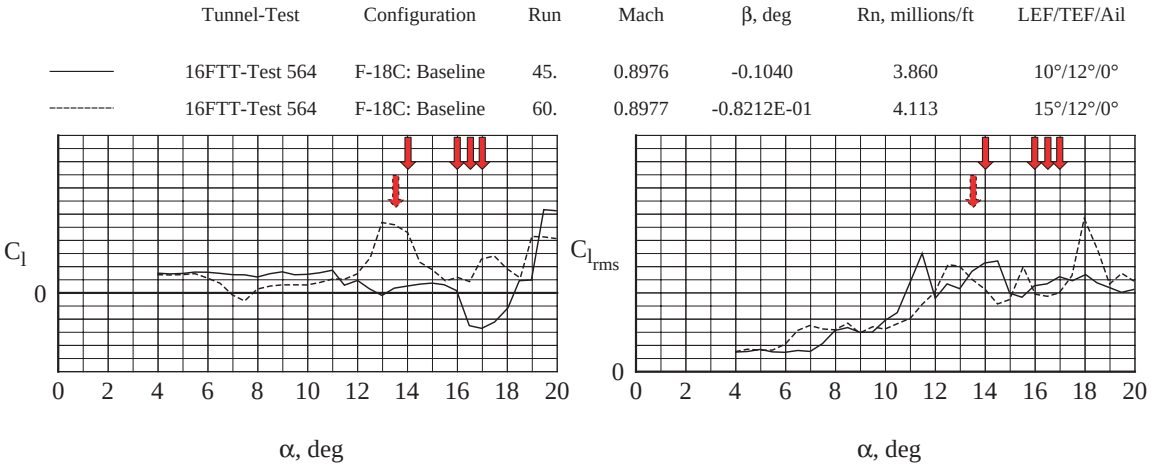

Figure 11. (b) Concluded.

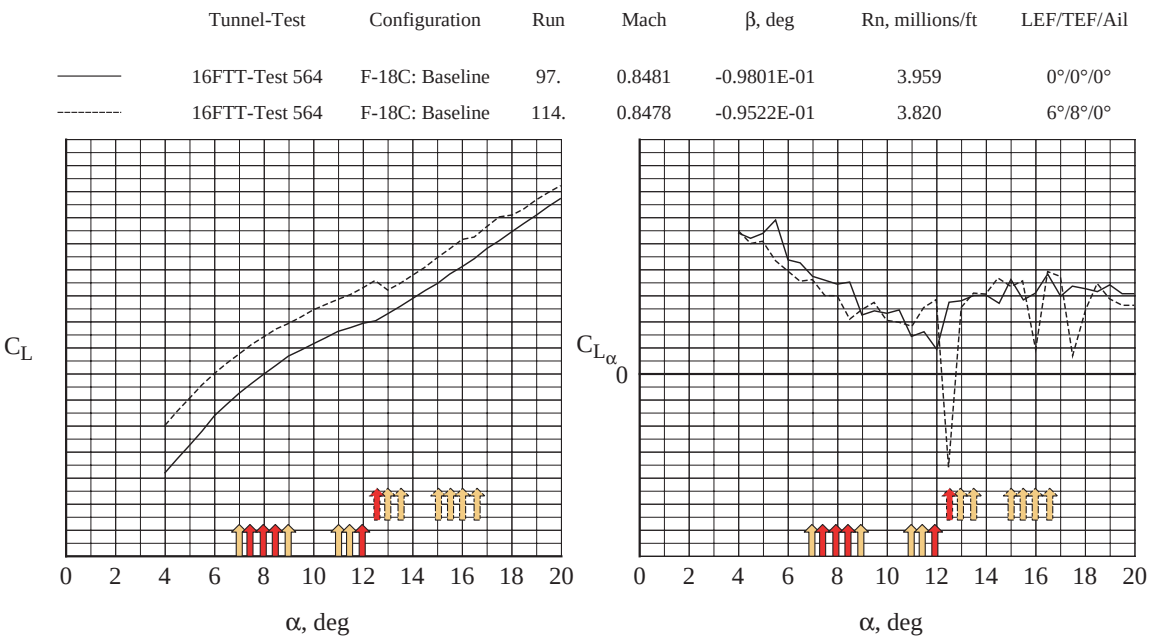

Figure 12. Lift and rolling moments with FTR data for the F/A-18C aircraft model at various flap settings and M = 0.85. (a) LEF/TEF/Ail at 0°/0°/0° and 6°/8°/0°.

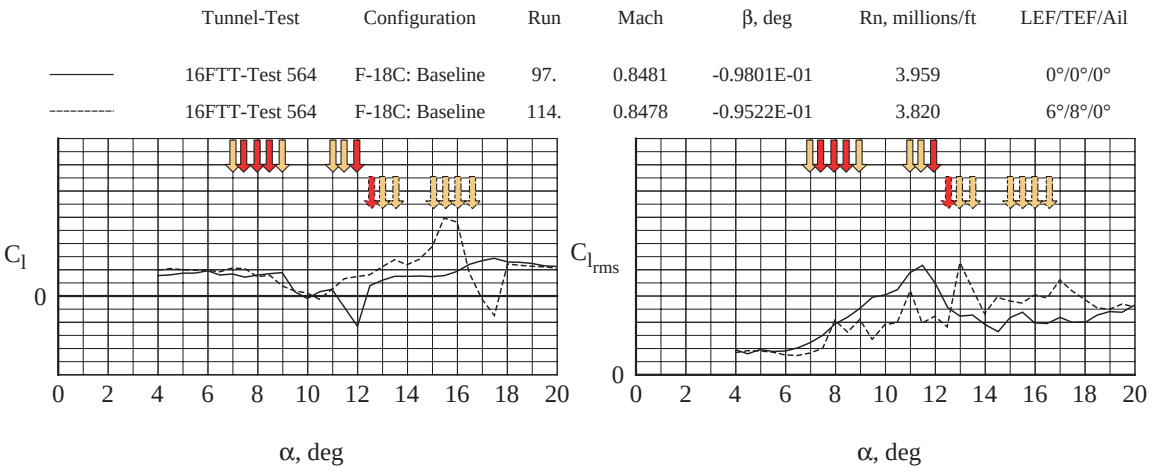

Figure 12. (a) Concluded.

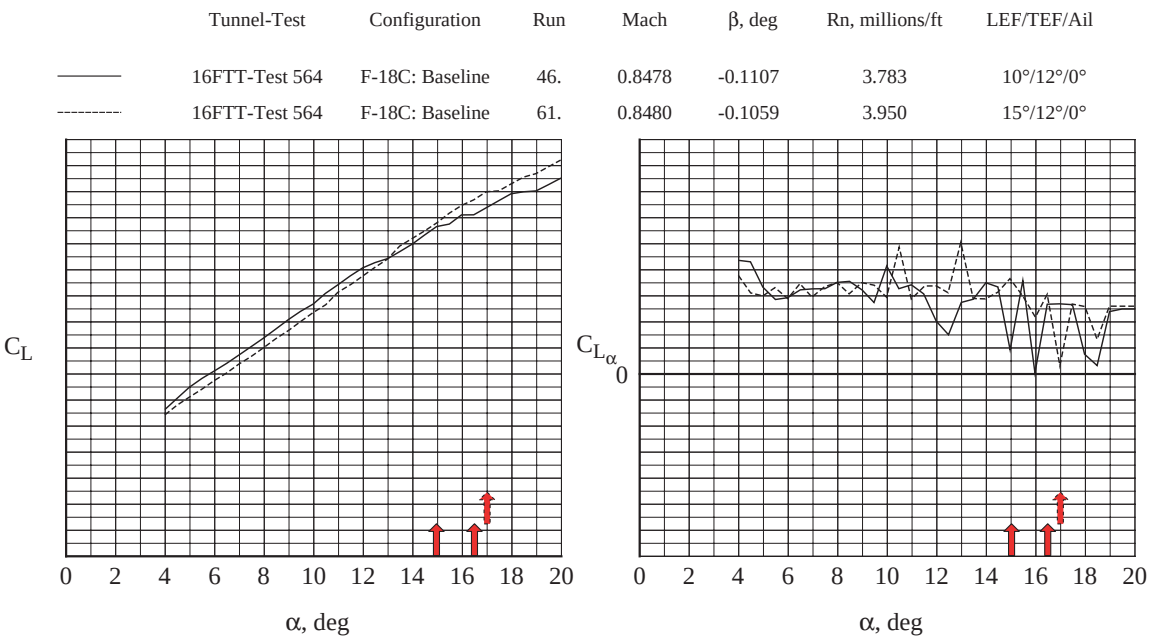

Figure 12. (b) LEF/TEF/Ail at 10º/12º/0º and 15º/12º/0º.

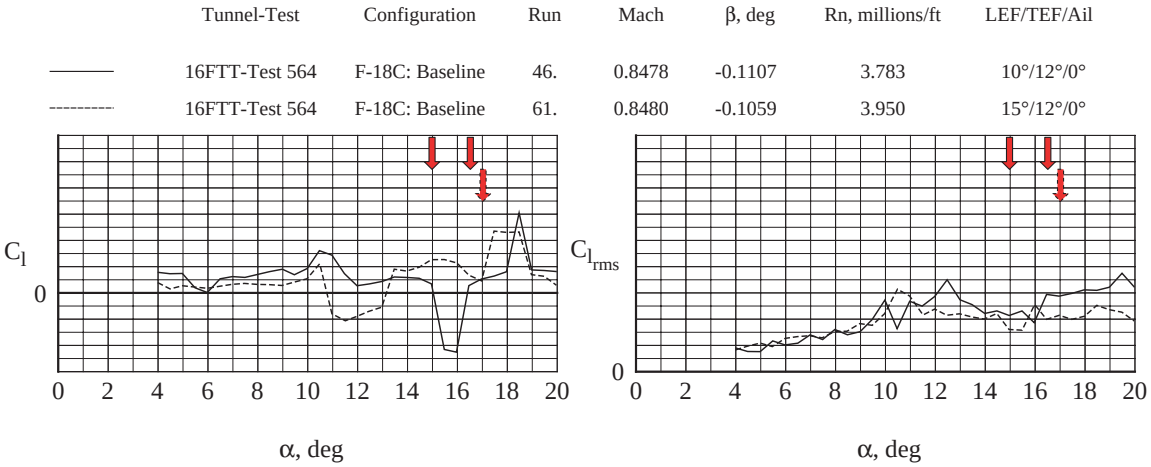

Figure 12. (b) Concluded.

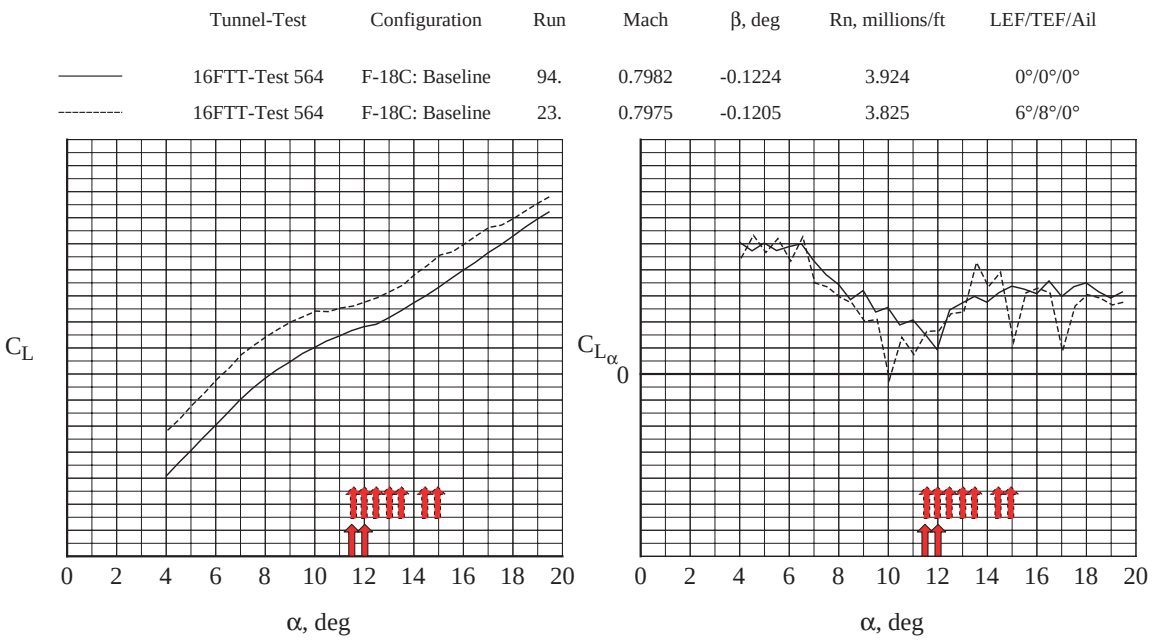

Figure 13. Lift and rolling moments with FTR data for the F/A-18C aircraft model at various flap settings and M = 0.8. (a) LEF/TEF/Ail at 0°/0°/0° and 6°/8°/0°.

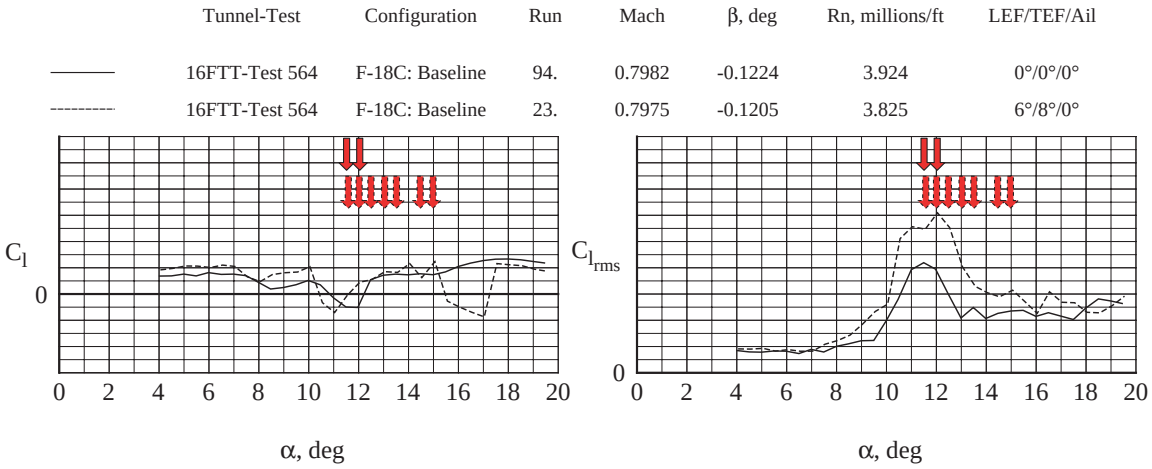

Figure 13. (a) Concluded.

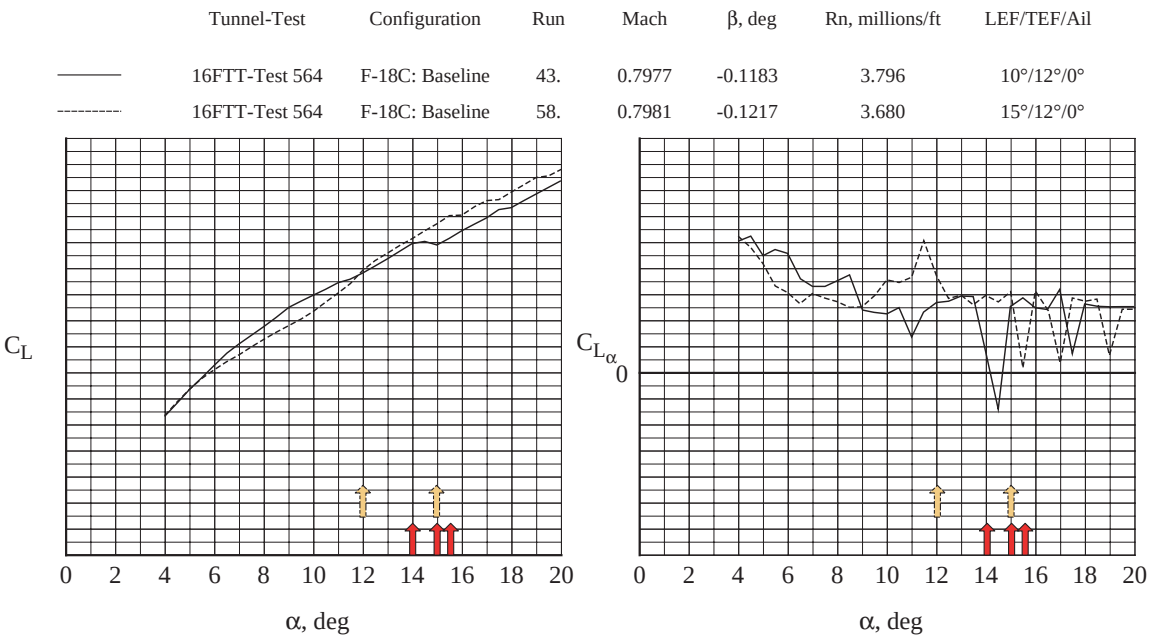

Figure 13. (b) LEF/TEF/Ail at 10°/12°/0° and 15°/12°/0°.

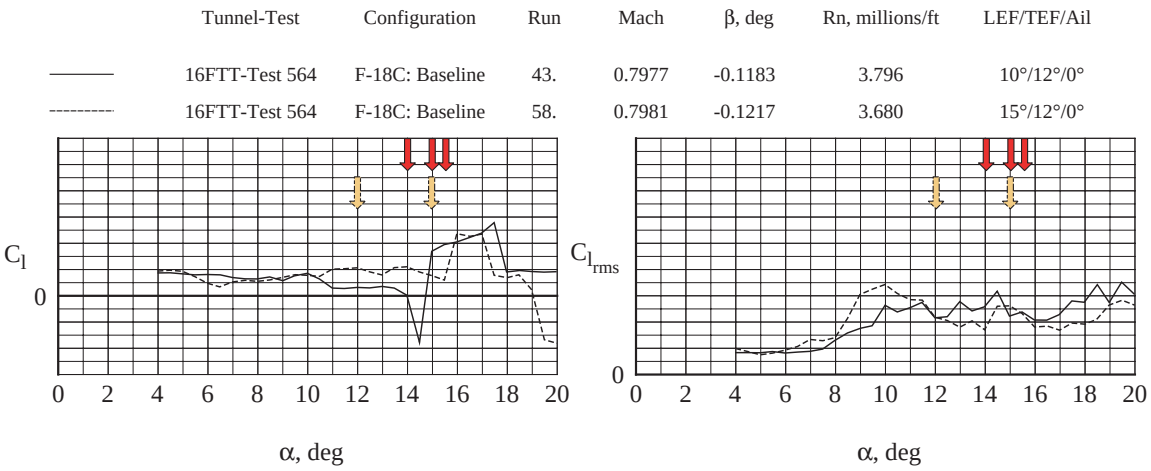

Figure 13. (b) Concluded.

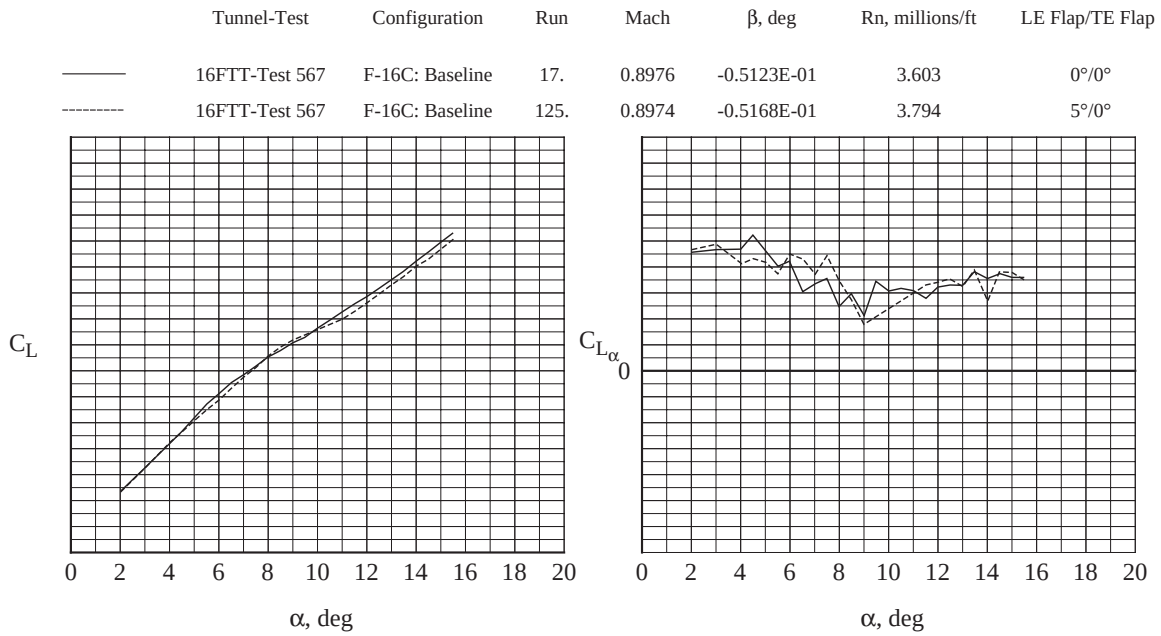

Figure 14. Lift, rolling- and wing-root-bending-moments with FTR data for the F-16C aircraft model at various flap settings and M = 0.9. (a) LEF/TEF at 0º/0º; 5º/0º.

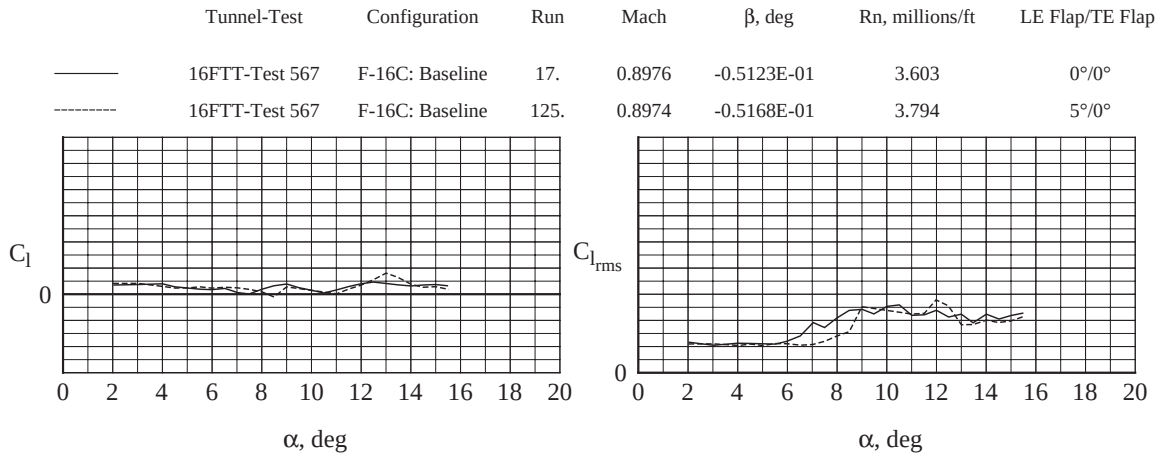

Figure 14. (a) Continued.

	Tunnel - Test	Configuration	Run	Mach	β, deg	Rn, millions/ft	LE Flap/TE Flap
———	16FTT-567	F-16C:Baseline	17.00	0.8977	-0.6054E-01	3.604	0°/0°
---------	16FTT-567	F-16C:Baseline	125.0	0.8974	-0.6188E-01	3.795	5°/0°

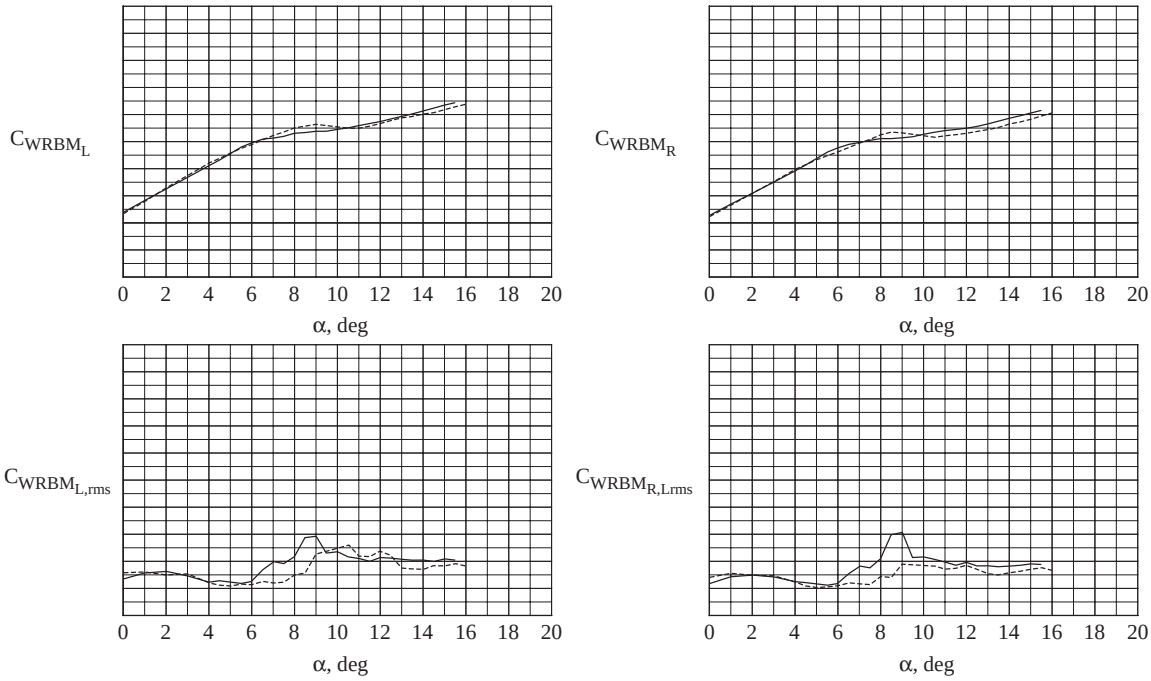

Figure 14. (a) Concluded.

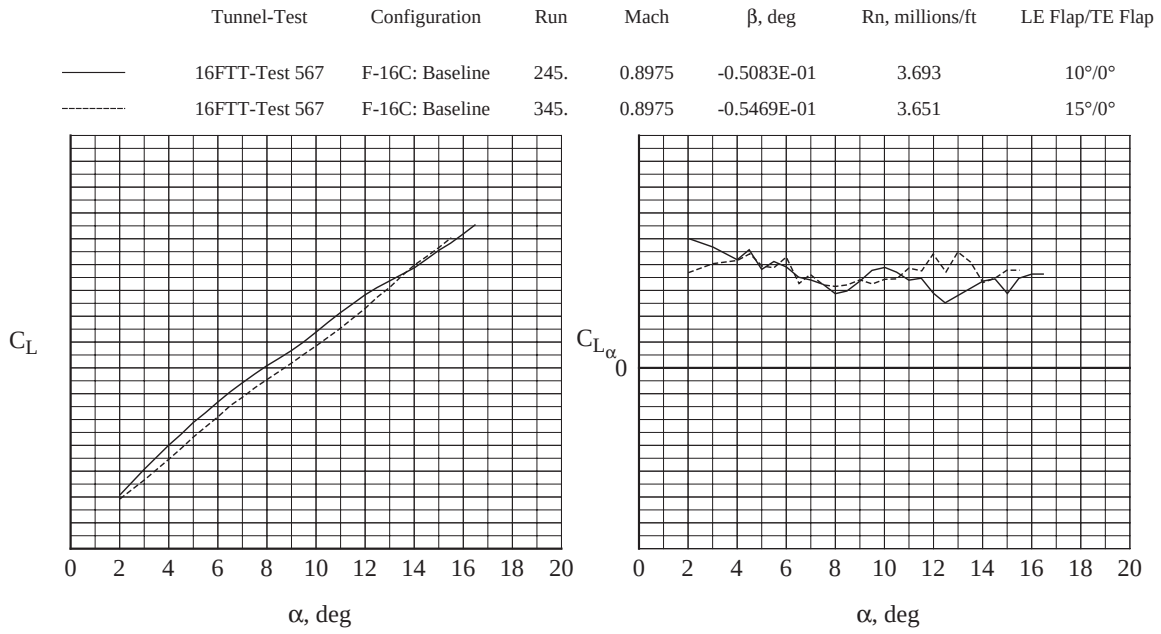

Figure 14. (b) LEF/TEF at $10^o/0^o$; $15^o/0^o$.

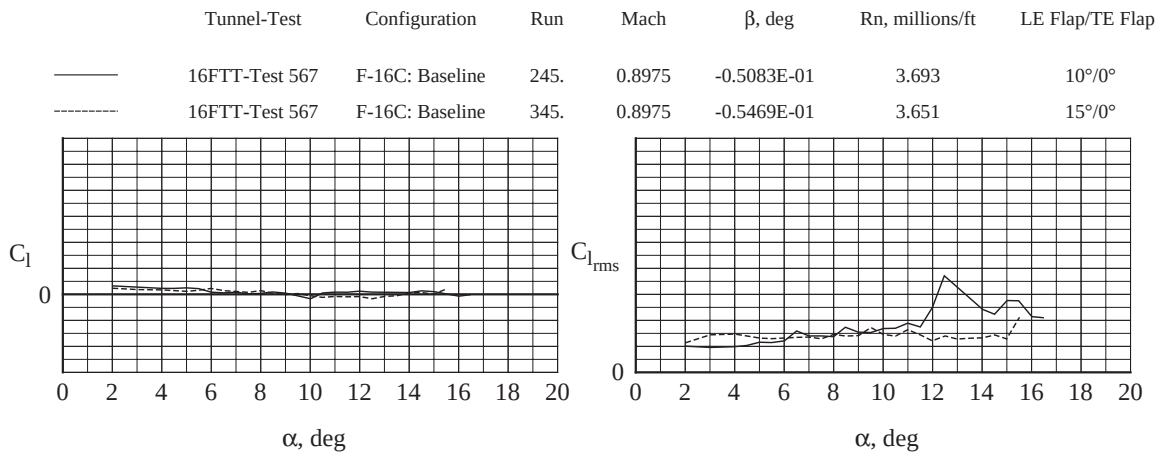

Figure 14. (b) Continued.

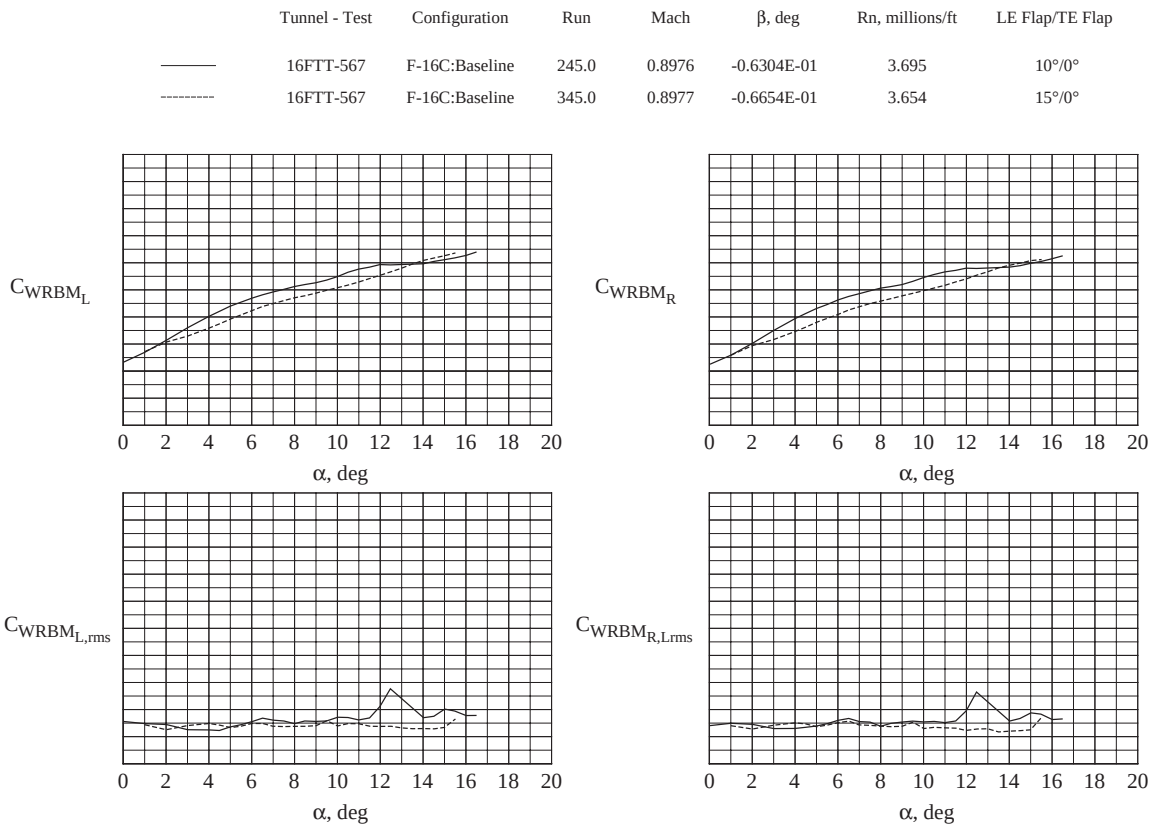

Figure 14. (b) Concluded.

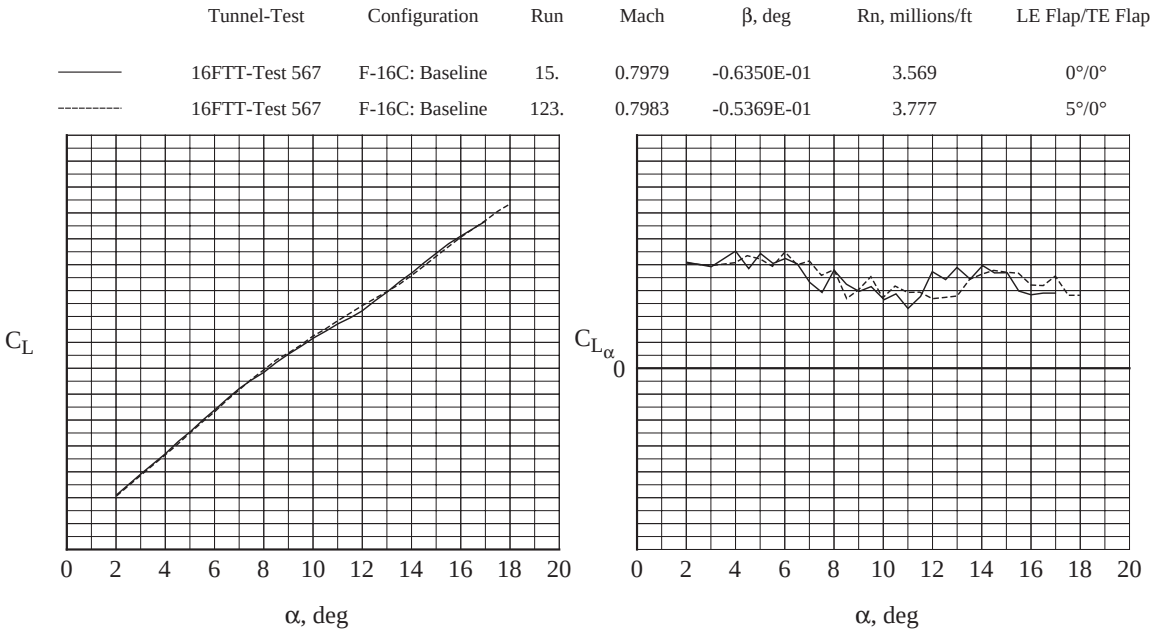

Figure 15. Lift, rolling- and wing-root-bending-moments with FTR data for the F-16C aircraft model at various flap settings and M = 0.8. (a) LEF/TEF at 0º/0º; 5º/0º.

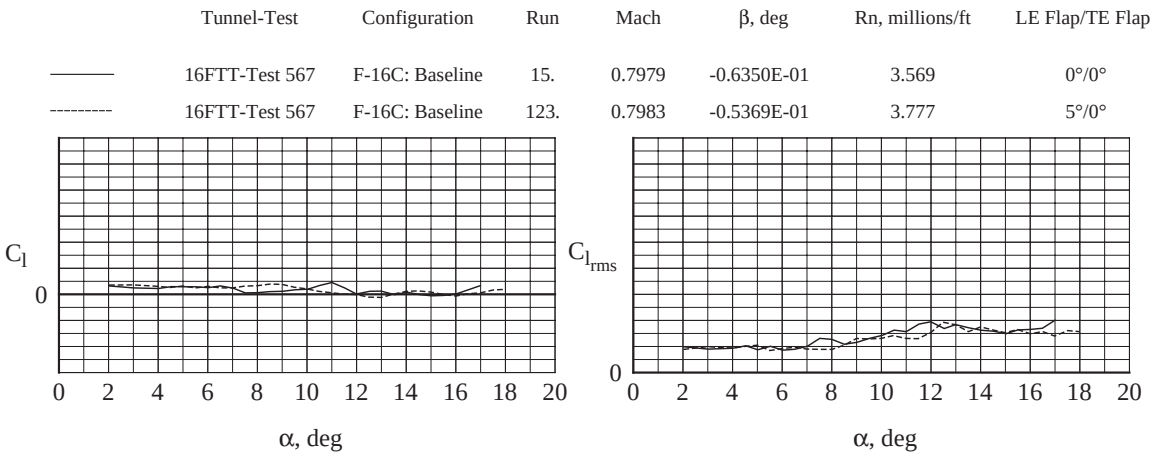

Figure 15. (a) Continued.

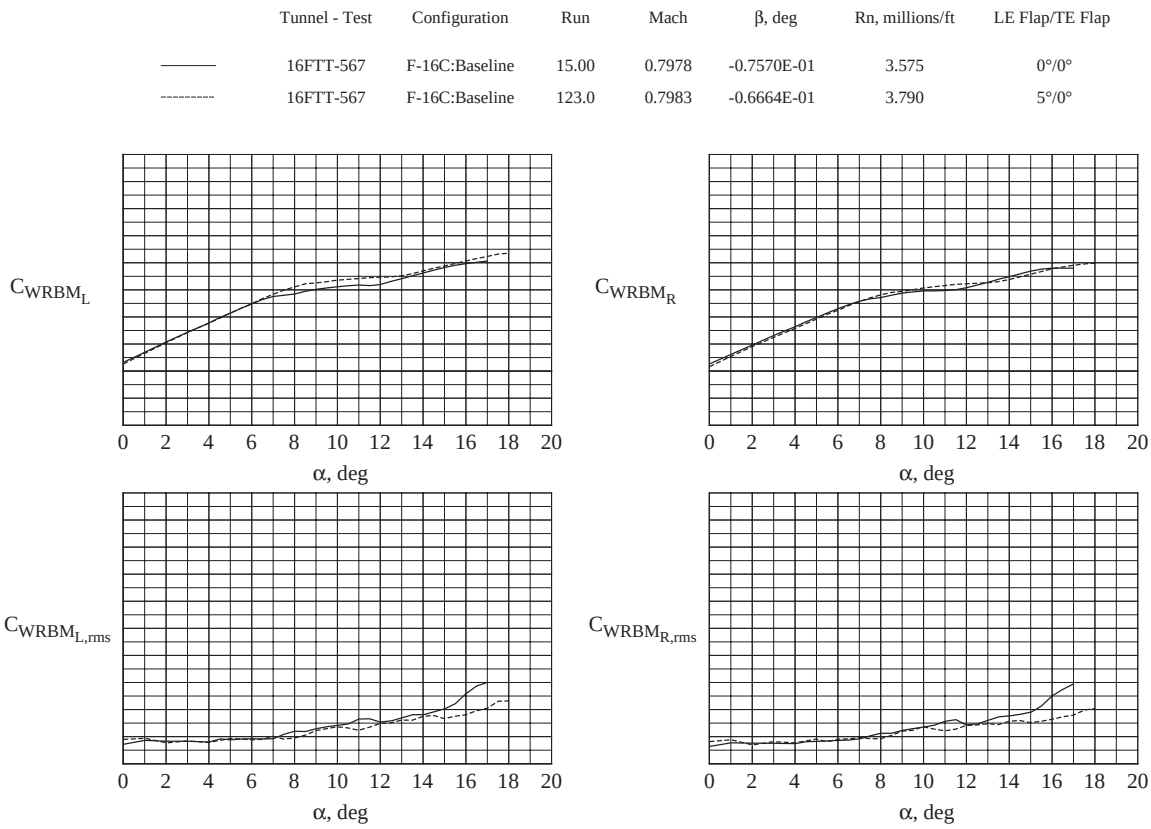

Figure 15. (a) Concluded.

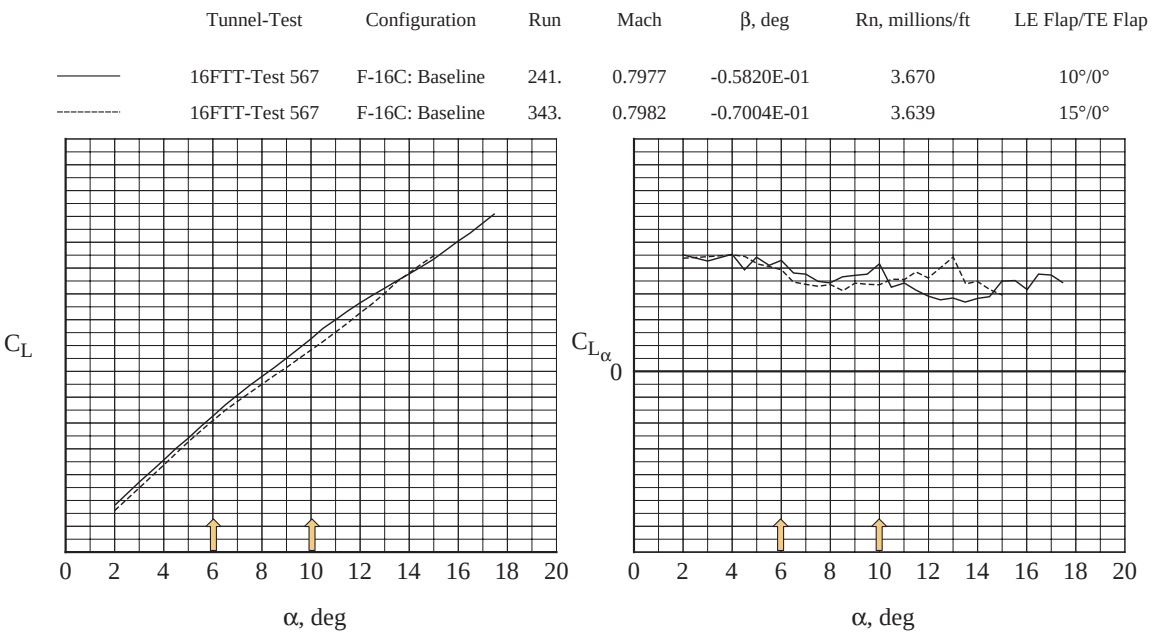

Figure15.(b) LEF/TEF at 10º/0º; 15º/0º.

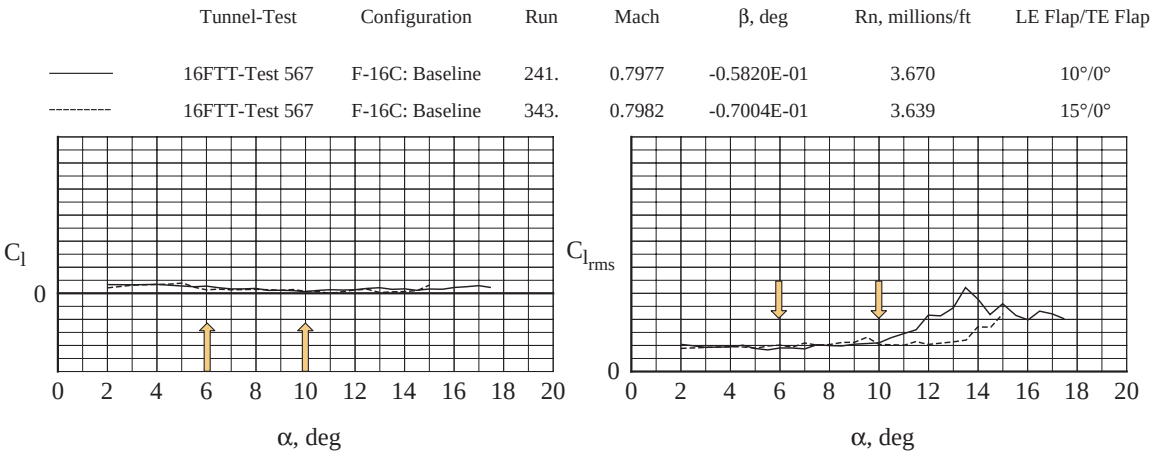

Figure 15. (b) Continued.

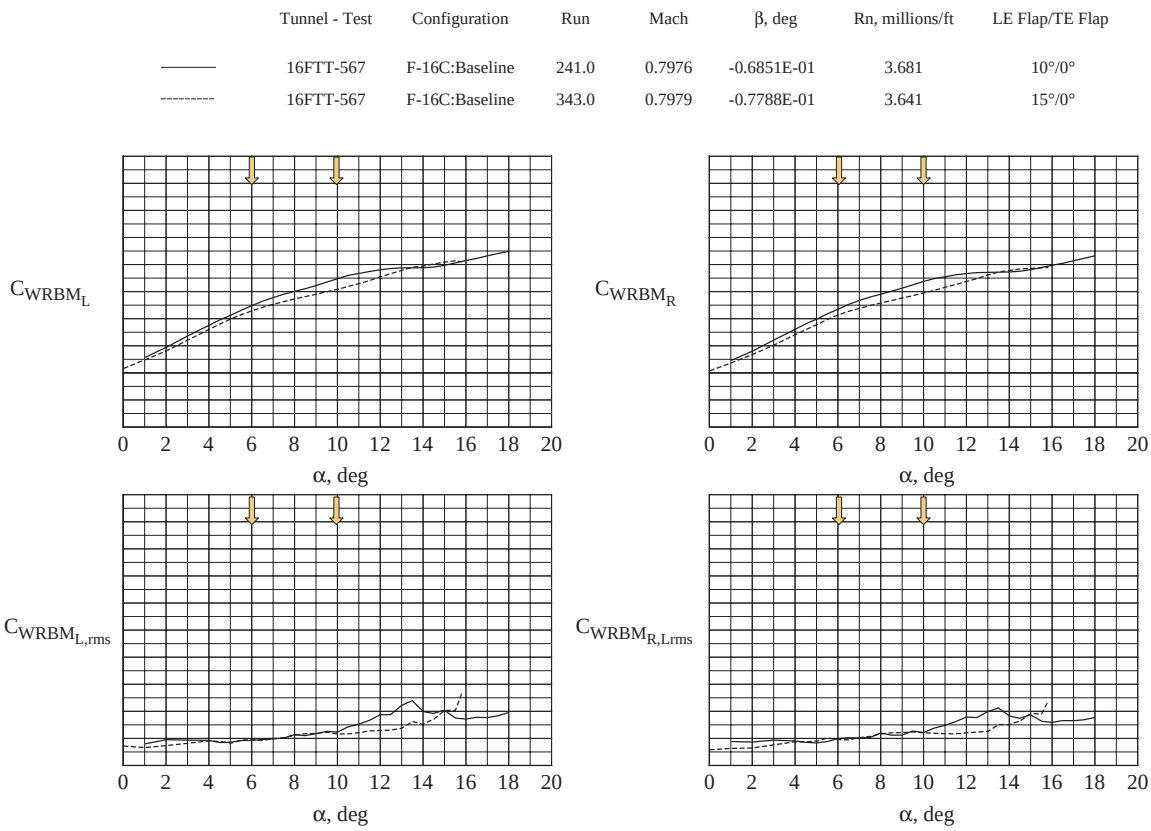

Figure 15. (b) Concluded.

Traditional FOMs – Ratings

Introduction of Tables

The results of the ratings (scorings) for each TFOM appear in three tables. Table 1 shows the details for each model, Mach number and flap set. Table 2 provides an initial summary for each model and Mach number by summing the individual flap results into a single ratio, whereas Table 3 summarizes all flap and Mach results into a single ratio for each configuration.

RATINGS FOR TRADITIONAL FIGURES OF MERIT

CONFIGURATION :

MACH NUMBER	LE	TE	Ail	C_L	$C_{L\alpha}$	C_l	$C_{l,rms}$	C_{WRBM}	$C_{WRBM,rms}$
F/A-18E: M=0.9	degs.	degs.	degs.						
	6	8	4	9(1)/9	9(2)/9	9(2)/9	8(0)/9	7(0)/9	8(0)/9
	10	10	5	5(2)/5	5(5)/5	5(2)/5	5(2)/5	4(0)/5	4(0)/5
	15	10	5	7(3)/7	7(6)/7	7(2)/7	7(1)/7	N/A	N/A
	20	10	0	4(4)/4	4(8)/4	4(0)/4	4(0)/4	N/A	N/A
F/A-18E: M=0.8									
	6	8	4	9(2)/9	9(5)/9	7(0)/9	9(0)/9	9(1)/9	9(1)/9
	10	10	5	3(3)/3	3(7)/3	1(3)/3	3(1)/3	3(2)/3	3(1)/3
	15	10	5	2(5)/2	2(7)/2	2(4)/2	2(1)/2	N/A	N/A
	20	10	0	5(2)/5	5(6)/5	5(1)/5	5(1)/5	N/A	N/A
AV-8B: M=0.75									
100% LERX	*****	10	*****	6(2)/6	6(2)/6	6(1)/6	6(0)/6	N/A	N/A
65% LERX	*****	10	*****	11(1)/11	11(2)/11	11(0)/11	11(0)/11	N/A	N/A
AV-8B: M=0.50									
100% LERX	*****	25	*****	0(3)/1	0(3)/1	1(1)/1	1(1)/1	N/A	N/A
	*****	15	*****	0(4)/0	0(3)/0	0(0)/0	0(1)/0	N/A	N/A
	*****	10	*****	0(4)/0	0(3)/0	0(0)/0	0(0)/0	N/A	N/A
65% LERX	*****	25	*****	7(3)/7	7(7)/7	7(2)/7	7(1)/7	N/A	N/A
	*****	10	*****	1(2)/1	1(1)/1	1(2)/1	1(1)/1	N/A	N/A
AV-8B: M=0.30									
100% LERX	*****	25	*****	6(3)/6	6(4)/6	6(2)/6	6(0)/6	N/A	N/A
65% LERX	*****	25	*****	10(2)/10	10(2)/10	10(2)/10	10(0)/10	N/A	N/A
F/A-18C: M=0.9									
	0	0	0	6(1)/7	7(4)/7	7(1)/7	7(1)/7	N/A	N/A
	6	8	0	2(2)/2	2(4)/2	2(3)/2	2(2)/2	N/A	N/A
	10	12	0	4(4)/4	2(7)/4	4(0)/4	4(1)/4	N/A	N/A
	15	12	0	1(5)/1	1(6)/1	1(3)/1	1(2)/1	N/A	N/A
F/A-18C: M=0.85									
	0	0	0	8(0)/8	8(5)/8	4(0)/8	8(0)/8	N/A	N/A
	6	8	0	7(3)/7	7(4)/7	7(1)/7	7(1)/7	N/A	N/A
	10	12	0	2(3)/2	2(6)/2	2(3)/2	1(2)/2	N/A	N/A
	15	12	0	2(2)/2	2(3)/2	2(1)/2	0(1)/2	N/A	N/A
F/A-18C: M=0.8									
	0	0	0	2(2)/2	2(0)/2	2(0)/2	2(0)/2	N/A	N/A
	6	8	0	7(4)/7	7(5)/7	7(0)/7	5(1)/7	N/A	N/A
	10	12	0	3(6)/3	3(5)/3	3(0)/3	3(1)/3	N/A	N/A
	15	12	0	2(4)/2	2(6)/2	1(1)/2	2(1)/2	N/A	N/A
F-16C: M=0.9									
	0	0	*****	0(4)/0	0(6)/0	0(2)/0	0(1)/0	0(4)/0	0(1)/0
	5	0	*****	0(4)/0	0(5)/0	0(2)/0	0(2)/0	0(4)/0	0(1)/0
	10	0	*****	0(5)/0	0(4)/0	0(0)/0	0(2)/0	0(4)/0	0(1)/0
	15	0	*****	0(4)/0	0(3)/0	0(0)/0	0(1)/0	0(3)/0	0(0)/0
F-16C: M=0.8									
	0	0	*****	0(4)/0	0(6)/0	0(2)/0	0(2)/0	0(5)/0	0(1)/0
	5	0	*****	0(3)/0	0(6)/0	0(0)/0	0(0)/0	0(3)/0	0(0)/0
	10	0	*****	2(2)/2	2(4)/2	0(0)/2	1(1)/2	2(2)/2	1(0)/2
	15	0	*****	0(3)/0	0(3)/0	0(0)/0	0(1)/0	0(3)/0	0(1)/0

NOTES: **Pattern of Table is: xx(yy)/zz**

N/A -- Not Available

where xx is the number of arrows within 1 degree AOA of an event
yy is the number of static events not indicate by arrows
zz is the number of red and yellow arrows

Table 1. Ratings of Traditional Figures of Merit for all four models at all test conditions.

SUMMARY -- RATINGS FOR TRADITIONAL FIGURES OF MERIT						
CONFIGURATION : MACH NUMBER	C_L	$C_{L\alpha}$	C_l	$C_{l,rms}$	C_{WRBM}	$C_{WRBM,rms}$
F/A-18E: M=0.9	25(10)/25	25(21)/25	25(6)/25	24(3)/25	11(0)/14	12(0)/14
F/A-18E: M=0.8	19(12)/19	19(25)/19	15(8)/19	19(3)/19	12(3)/12	12(2)/12
AV-8B: M=0.75	17(3)/17	17(4)/17	17(1)/17	17(0)/17	N/A	N/A
AV-8B: M=0.50	8(16)/9	8(17)/9	9(5)/9	9(4)/9	N/A	N/A
AV-8B: M=0.30	16(5)/16	16(6)/16	16(4)/16	16(0)/16	N/A	N/A
F/A-18C: M=0.9	13(12)/14	12(21)/14	14(7)/14	14(6)/14	N/A	N/A
F/A-18C: M=0.85	19(8)/19	19(18)/19	15(5)/19	16(4)/19	N/A	N/A
F/A-18C: M=0.8	14(16)/14	14(16)/14	13(1)/14	12(3)/14	N/A	N/A
F-16C: M=0.9	0(17)/0	0(18)/0	0(4)/0	0(6)/0	0(15)/0	0(3)/0
F-16C: M=0.8	2(12)/2	2(19)/2	0(2)/2	1(4)/2	2(13)/2	1(2)/2

NOTES: Pattern of Table is: xx(yy)zz — N/A -- Not Available
where xx is the number of arrows within 1 degree AOA of an event
yy is the number of static events not indicated by arrows
zz is the number of red and yellow arrows

Table 2. Summary of Traditional Figures of Merit Ratings for all four models by Mach number.

CONFIGURATIONAL SUMMARY RATINGS FOR TRADITIONAL FIGURES OF MERIT						
CONFIGURATION	C_L	$C_{L\alpha}$	C_l	$C_{l,rms}$	C_{WRBM}	$C_{WRBM,rms}$
F/A-18E	44(22)/44	44(46)/44	40(14)/44	43(6)/44	23(3)/26	24(2)/26
AV-8B	41(24)/42	41(27)/42	42(10)/42	42(4)/42	N/A	N/A
F/A-18C	46(36)/47	45(65)/47	42(13)/47	42(13)/47	N/A	N/A
F-16C	2(29)/2	2(37)/2	0(6)/2	1(10)/2	2(28)2	1(5)/2

NOTES: Pattern of Table is: xx(yy)zz — N/A -- Not Available
where xx is the number of arrows within 1 degree AOA of an event
yy is the number of static events not indicated by arrows
zz is the number of red and yellow arrows

Table 3. Traditional Figures of Merit Ratings summary by configuration. (This table is a summary of Table 2.)

Discussion of TFOMs Ratings

The best score a TFOM could achieve in any table would be of the form 50(0)/50; which amounts to 100% agreement with no missed flags. Table 1 shows about half of the items to have 100% agreement but only a small fraction of these have no misses. Tables 2 and 3 generally show a high percentage of agreement between the two data sets. However, Table 3 shows that even with this agreement the TFOM $C_{L\alpha}$ has the largest number of misses of any parameter. The TFOMs with the fewest overall misses are the C_l, $C_{l,rms}$, C_{WRBM} (excluding the F-16C data), and $C_{WRBM,rms}$ terms.

Even with good agreement overall, the TFOMs can give indications of FTR activity not validated by the response data, i.e., false positives.

Discussion of TFOM Results

Three questions remain. The first is: Can you rely upon any TFOM to discern whether a new airplane model will experience an AWS event with certainty? This a restatement of the necessary and sufficient condition question raised previously. The second is: Does the TFOM data lead or lag the FTR response data? The third is: Do any of these TFOMs help to sort the two sets of configurations into those which will likely have AWS events from those which will unlikely?

The answer to the first question is NO, not with 100% certainty, based on these four model tests. Particular TFOMs indicate merely necessary conditions but they are not always sufficient. The TFOMs can almost be considered conservative, yielding more flags than events, however they also miss events recorded by the FTR response data. Thus, if you can only employ one test technique to assess AWS events, use the FTR rig.

The answer to the second question is the same as stated in the section entitled **Example Results Summary**. There appears to be no general pattern of one data type leading or lagging the other. The leading or lagging results are configuration, flap-set and Mach number dependent. For example, with some combinations of models and Mach numbers, the $C_{L\alpha}$ data do indicate an increase in value followed by a decrease within an α range of 5^o in the vicinity of the FTR arrows; whereas, the opposite behavior is true for others.

Regarding the third question about configuration sorting, an examination of the TFOMs in Figures 6 to 15 was made. The result is that all four models would be expected to have some AWS events based on the stringent criteria established. So even though the TFOMs don't sort out the models perfectly, they are still very useful. Hence, all TFOMs should be employed in future tests in order to document those flagged features that have historically been associated with AWS events.

A related question is did the FTR response data sort the models into two groups? Based on counting the arrows for each configuration, the answer is that this technique sorted three of the models — the two known for AWS events, the pre-production F/A-18E and the AV-8B at the extremes of its flight envelope with the F/A-18C, flaps not on

schedule — into the AWS group and the F-16C into the non-AWS group.

ALTERNATE FOM STUDIES

Background

Since none of the traditional FOMs works with 100% accuracy with no misses, alternative FOMs (AFOMs) were considered to determine whether they could offer improvement. The AFOMs considered occur in two different groups, unsteady and static, and both can use combinational forms to help distinguish between AWS and non-AWS events.

The unsteady group incorporates the rms components of selected aerodynamic terms, whereas, the static deals with the derivative form of basic aerodynamic coefficients.

Unsteady

This group of Alternate FOMs is based on an observation that during a prior test (16FTT – Test 523) of the pre-production F/A-18E model, it became active in the pitch-plunge mode in the α range where AWS events were occurring. This lead to a hypothesis that the lateral and longitudinal components of a wind-tunnel model can respond to flow-separation and unsteadiness in both the roll and pitch axes and can be identified from the balance rms signals. The signals identified as being relevant for this model were $C_{WRBM,rms}$, $C_{l,rms}$, and $C_{N,rms}$. Since $C_{WRBM,rms}$ and $C_{l,rms}$ have already been discussed, an example is given in Figure 16 from this prior test as to why there should be a focus on $C_{N,rms}$.

Of interest here is to understand whether the severity of AWS events is related to $C_{N,rms,}$, in particular for this model. Once lessons have been learned for the pre-production F/A-18E, these are applied to the other configurations in order to ascertain the generality.

	Tunnel-Test	Configuration	Run	M_∞	β, deg	Rn, millions/ft	LEF/TEF/Ail
———	16FTT-523	F/A-18E: Baseline	72.	0.8990	-0.1201	3.706	6°/8°/4°
----------	16FTT-523	F/A-18E: Baseline	176.	0.9000	-0.1196	3.721	10°/10°/5°
———--	16FTT-523	18-inch ISE	257.	0.8998	-0.1179	3.915	10°/10°/5°

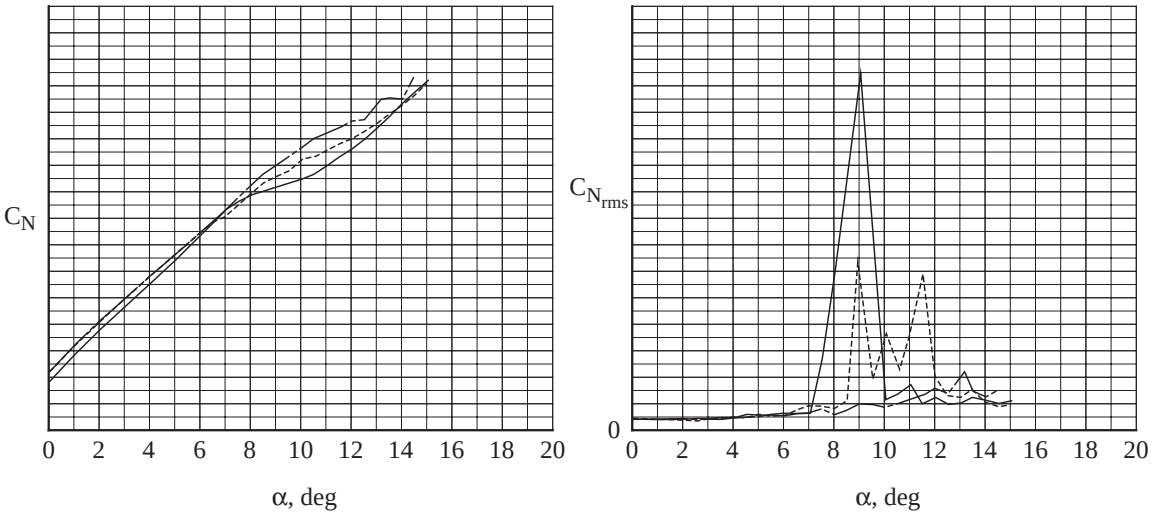

Figure 16. C_N and $C_{N,rms}$ for three variations of the pre-production F/A-18E model at two Mach numbers. (a) M = 0.9.

	Tunnel-Test	Configuration	Run	M_∞	β, deg	Rn, millions/ft	LEF/TEF/Ail
———	16FTT-523	F/A-18E: Baseline	53.	0.7987	-0.1286	3.696	6°/8°/4°
----------	16FTT-523	F/A-18E: Baseline	163.	0.7997	-0.1274	3.722	10°/10°/5°
———--	16FTT-523	18-inch ISE	251.	0.7992	-0.1271	3.791	10°/10°/5°

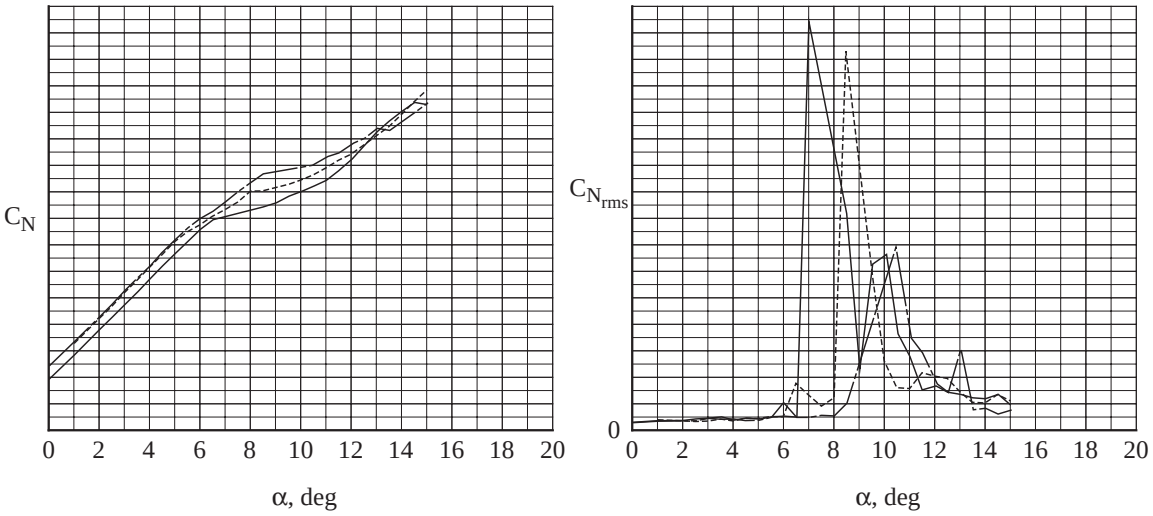

Figure 16. (b) M = 0.8.

These prior experiments had as a goal the identification of some aerodynamic parameter or combination of parameters that would be a reliable FOM predictor for AWS events on the pre-production F/A-18E. At the time of these wind-tunnel tests no FTR data existed but flight data did, so the latter became the standard. Flight data are very useful and from an assessment of the records it was noted that with certain configurational variations on the aircraft, the AWS events were delayed until a higher value of α. There were three aircraft variations, with the first two differing only in the Flight Control Law. They are designated (a) FCLv.6.0.2 (simulated in wind-tunnel by the $6^o/8^o/4^o$ LE/TE/Ail flap settings), (b) FCLv.6.1.3 (simulated by the $10^o/10^o/5^o$ flap settings), and (c) same FCL as (b) but with an 18"Inboard Snag Extension (ISE). [The FCLv6.1.3 was noted by test pilots as the "80% solution" to the AWS problem.] AWS events occurred at higher values of α in going from (a) to (c), so parameters were sought which would show the same order of improvement, although not necessarily at the same flight α values.

The $C_{N,rms}$ vs. α curves for these three variations (Fig. 16), tend to develop significant activity in the same α order as found in flight. This is encouraging and, consequently, could lead to the $C_{N,rms}$ being considered a potential FOM.

Since no one TFOM has yielded 100% agreement with no misses in Table 3 for this model, it is useful to consider combining the $C_{N,rms}$ parameter with two of the more successful TFOMs; namely, $C_{l,rms}$ and C_l, or ΔC_l— this term ($\equiv C_{l|\alpha} - C_{l|\alpha=0^o}$) is used to remove any C_l offset present at low values of α. Two different means of combination are employed, one is an rms weighted sum called, ΣFOM,3 – the original form, and the other is the absolute value of a simple product, ΠFOM. The equations used to compute these two terms follow and the results are plotted in Figure 17.

$$\Sigma FOM,3 = \sqrt{(A1*C^2_{N,rms}+A2*C^2_{l}+A3*C^2_{l,rms})/3}$$: |Reference 11 uses a simplified form for $\Sigma FOM,3=\sqrt{(C^2_{N,rms}+C^2_{l}+C^2_{l,rms})/3}$.

where for the Langley 16FTT Test 523, the values are:
A1 = 1/(.051)**2,
A2 = 1/(.0014)**2, and
A3 = 1/(.0084)**2. These coefficients have been normalized by the corresponding values at the $10^o/10^o/5^o$ flaps at M = 0.90 and $\alpha = 9.0°$.

and

$$\Pi FOM = | C_{N,rms} \times C_{l,rms} \times \Delta C_l |$$

	Tunnel-Test	Configuration	Run	M_∞	β, deg	Rn, millions/ft	LEF/TEF/Ail
———	16FTT-523	F/A-18E: Baseline	72	0.8990	-0.1191	3.706	6°/8°/4°
- - - - - - - - -	16FTT-523	F/A-18E: Baseline	176	0.9000	-0.1187	3.721	10°/10°/5°
——– – –	16FTT-523	18-inch ISE	250	0.8997	-0.1198	3.911	10°/10°/5°

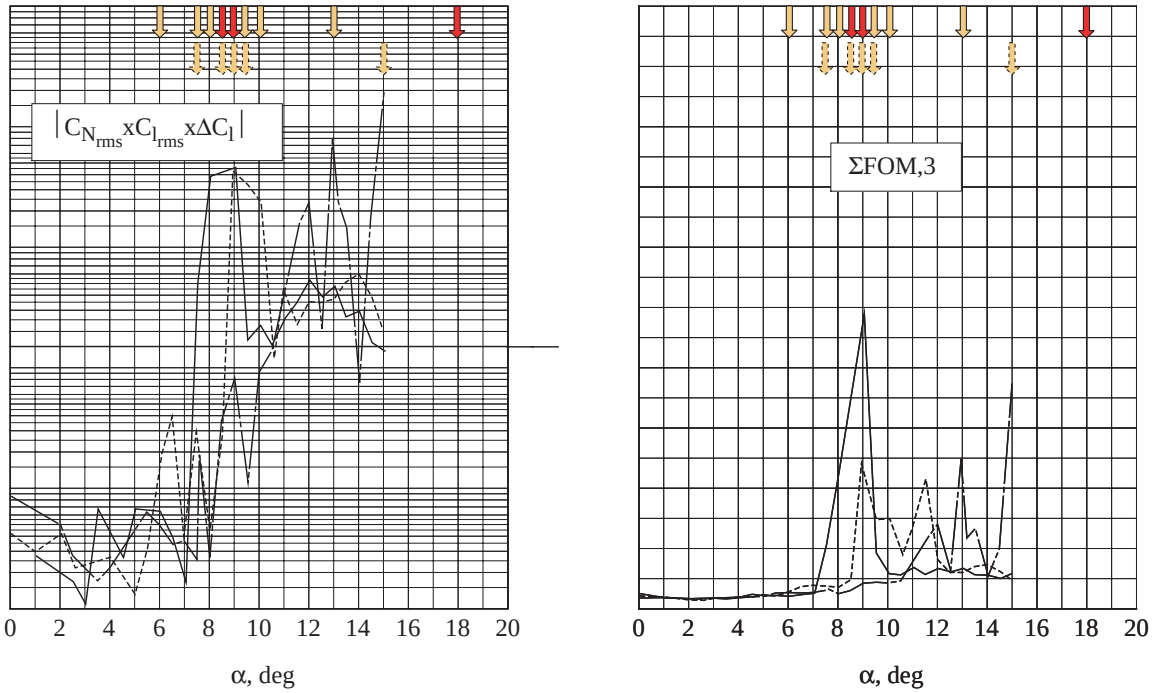

Figure 17. Two FOMs based on a combination of steady and unsteady results for the pre-production F/A-18E with geometry variations at two Mach numbers. (a) M = 0.9.

	Tunnel-Test	Configuration	Run	M_∞	β, deg	Rn, millions/ft	LEF/TEF/Ail
———	16FTT-523	F/A-18E: Baseline	53	0.7987	-0.1281	3.696	6°/8°/4°
----------	16FTT-523	F/A-18E: Baseline	163	0.7997	-0.1270	3.721	10°/10°/5°
———-–	16FTT-523	18-inch ISE	251	0.7992	-0.1266	3.791	10°/10°/5°

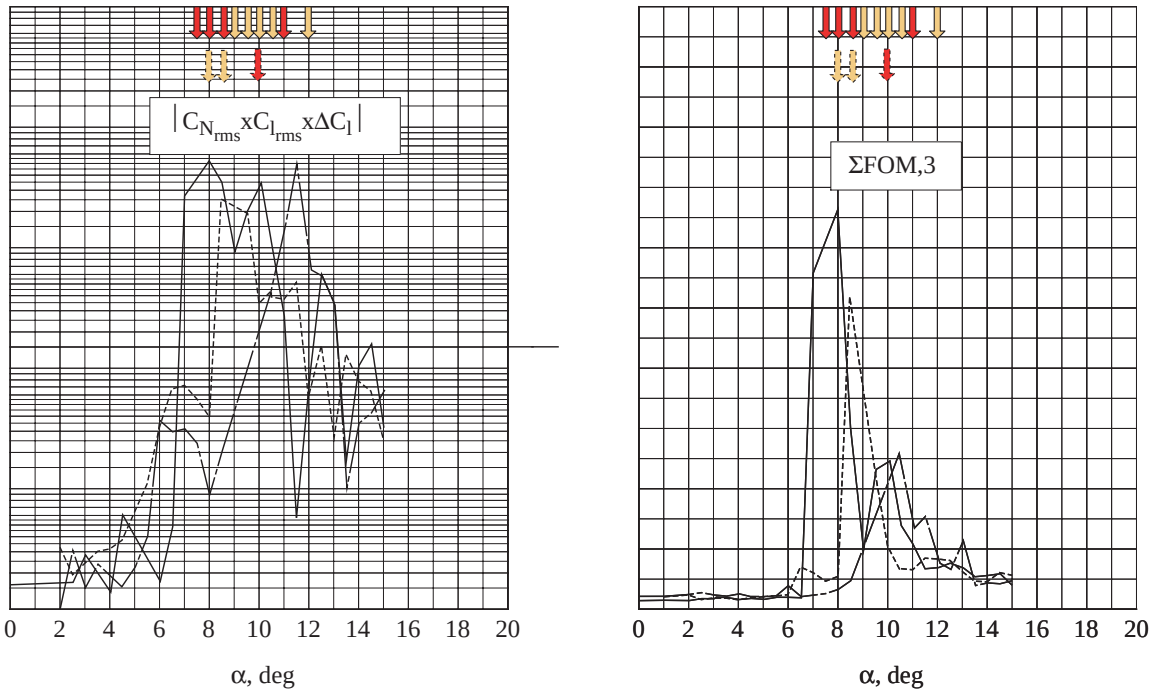

Figure 17. (b) M = 0.8.

<u>Alternative FOM-Unsteady Ratings</u>

<u>Criteria for AFOM Agreement</u>

There is a need to define success or matching between the FTR response data and the static data for each of these two AFOMs; i.e., establish a criterion. A match for the ΠFOM parameter is defined to occur if the ΠFOM value remains above the horizontal line at values of α which are within 1° from an arrow. (This horizontal line was found useful in sorting pre-production F/A-18E model configurations from different wind-tunnels and Mach numbers in a manner that matched the same order as determined in flight for an increase in α before the first occurrence of an AWS event. See the ***<u>Configuration Ordering of AWS Flight Events</u>*** section for a further discussion.) For the ΣFOM,3 parameter a match occurs if <u>any portion of an spike (static-data flagged feature)</u>, regardless of its size, happens at an α which is within 1° from an arrow.

[The reader is again reminded that the original version of ΣFOM,3 differs fromthe simplified version used in Reference 11.]

RATINGS FOR ALTERNATIVE FIGURES OF MERIT		
CONFIGURATION	**Π FOM**	**Σ FOM,3**
F/A-18E(Pre-Prod.)	**23(0)/26***	**24(0)/26***
AV-8B(Env.Extrm.)	**46(44)/49**	**N/A**
F/A-18C	**39(95)/47**	**N/A**
F-16C	**0(10)/2**	**N/A**

*** Only the 6/8/4 and 10/10/5 flap sets are considered here.**

Pattern of Table is: xx(yy)zz
where xx is the number of arrows within 1 degree AOA of an event
yy is the number of static events not indicated by arrows
zz is the number of red and yellow arrows

Table 4. Sum of Alternative FOM-Unsteady Ratings for all Mach-number and flap-set combinations*.

Discussion of AFOM-Unsteady Ratings

Based on these definitions for ΠFOM and ΣFOM,3, Table 4 has been prepared for these four models; however, the emphasis here will be on the data for the pre-production F/A-18E shown in Figure 17. Note that ΠFOM and ΣFOM,3 have a success rate of 88% and 92%, respectively, with no misses for the two flap-set ($6^o/8^o/4^o$ & $10^o/10^o/5^o$) and Mach-number (0.9 & 0.8) combinations. These ratings could perhaps have been higher in that the α limit for this test was $\approx 15^o$ and there was one arrow at $\alpha = 18^o$ for M = 0.9. [No 18" ISE configuration FTR response data is available for comparison.] Table 1 shows that for this model with the same test combinations, the C_L and $C_{L\alpha}$ TFOMs to have a 100% success rate. However, they had misses of eight and nineteen, respectively. The other TFOMs in this set, C_l, $C_{l,rms}$, C_{WRBM} and $C_{WRBM,rms}$, have a success rate of 85% with seven misses, 96% with three misses, 85% with three misses and 92% with two misses; respectively.

Table 4 is thus encouraging for the pre-production F/A-18E model. However, applying the same ΠFOM strategy – including using the same value as that for the pre-production F/A-18E, i.e., the horizontal line, – to the other models listed in the table yielded no general improvement over the TFOMs at estimating AWS events. [Plotted comparisons are not shown but see Reference 11 for chart comparisons.]

Moreover, the ΠFOM rating, in terms of misses, is actually worse than any of the TFOMs for the F/A-18C configuration.

The values of A1, A2 and A3 needed in the original formulation of ΣFOM,3 parameter have not been developed for each configuration, so these AFOM results are not available. However, it is suspected that since both of these AFOMs use the $C_{N,rms}$ parameter, the ΣFOM,3 will do no better. The test data for the F/A-18C model provide an example which substantiates this statement. In particular, this model developed a pitch-plunge motion on the FTR rig (associated with $C_{N,rms}$) with no corresponding activity triggered in the roll mode. Thus, neither of the AFOMs-Unsteady parameters can be considered as a static FTR equivalent answer.

Configuration Ordering of AWS Flight Events

There was another purpose for establishing these AFOMs (ΠFOM and ΣFOM,3) and that was to determine if these combinations were capable of sorting configurations for AWS improvement. To that end, it should be noted that both the ΠFOM and ΣFOM,3 show a delay in what is considered AWS activity until a higher value of α as the configurations vary from (a) to (c), the same progression noted in flight.

Similar studies with other models in this test group should be undertaken.

Static

The static analysis begins from an understanding that the rolling-moment can be represented as an expansion about some test-point in either the prime wind-tunnel variables (θ and ϕ) or derived variables (α and β) as

$$C_{l|\theta,\phi} = C_{l,0} + [C_{l\phi} * \phi] + \text{dynamic terms}^{10}$$

or

$$C_{l|\alpha,\beta} = C_{l,0} + [C_{l\alpha} * \alpha + C_{l\beta} * \beta] + \text{dynamic terms}^{12}.$$

Obviously, only the $C_{l,0}$ and the [ ] terms can be determined from a static test, but the latter group represents the "spring component" in the equation of motion for roll. The combination of offset ($C_{l,0}$) and spring component is important in understanding the potential for restoring a configuration to a nominal position during either FTR or flight testing. (Simulator studies[13] have shown the important role that $C_{l,0}$ plays in the tendency of an aircraft to develop an AWS event.)

Both the $C_{l\alpha}$ and the $C_{l\beta}$ terms are of interest, but the latter term will be highlighted as it is a key lateral static-stability term (negative values for positive stability). Experimentally, the $C_{l\beta}$ term is obtained by differencing the C_l data taken at $\beta = \pm 2^o$. A sample of this is shown in Figure 18 and the resulting curve of $C_{l\beta}$ vs. α is shown in Figure 19 along with the corresponding $C_{L\alpha}$ curve.

	Tunnel-Test	Configuration	Run	M_∞	β, deg	Rn, millions/ft	LEF/TEF/Ail
———	16FTT-523	F/A-18E/F: Baseline	62.	0.8992	1.989	3.834	6°/8°/4°
----------	16FTT-523	F/A-18E/F: Baseline	72.	0.8990	-0.1199	3.706	6°/8°/4°
———--	16FTT-523	F/A-18E/F: Baseline	63.	0.8991	-1.992	3.835	6°/8°/4°

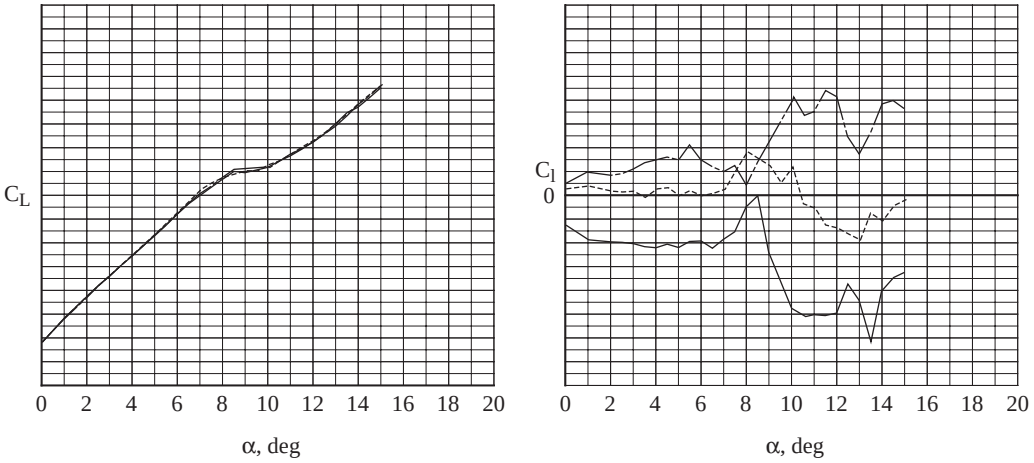

Figure 18. Effect of β on lift and rolling-moment data for the F/A-18E pre-production aircraft model at various Mach numbers and flap settings. (a) M = 0.9 and LEF/TEF/Ail at $6^o/8^o/4^o$.

	Tunnel-Test	Configuration	Run	M_∞	β, deg	Rn, millions/ft	LEF/TEF/Ail
———	16FTT-523	F/A-18E/F: Baseline	169.	0.8994	1.989	3.820	10°/10°/5°
---------	16FTT-523	F/A-18E/F: Baseline	176.	0.9000	-0.1196	3.721	10°/10°/5°
———--	16FTT-523	F/A-18E/F: Baseline	170.	0.8994	-1.995	3.762	10°/10°/5°

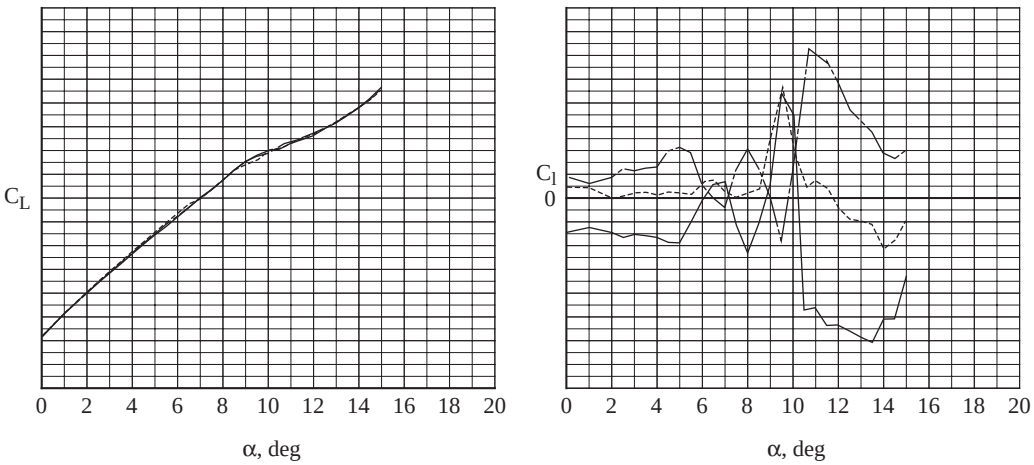

Figure 18. (b) M = 0.9 and LEF/TEF/Ail and$10^o/10^o/5^o$.

	Tunnel-Test	Configuration	Run	M_∞	β, deg	Rn, millions/ft	LEF/TEF/Ail
———	16FTT-523	F/A-18E/F: Baseline	55.	0.7996	2.001	3.669	6°/8°/4°
---------	16FTT-523	F/A-18E/F: Baseline	53.	0.7987	-0.1286	3.696	6°/8°/4°
———––	16FTT-523	F/A-18E/F: Baseline	54.	0.7992	-2.022	3.672	6°/8°/4°

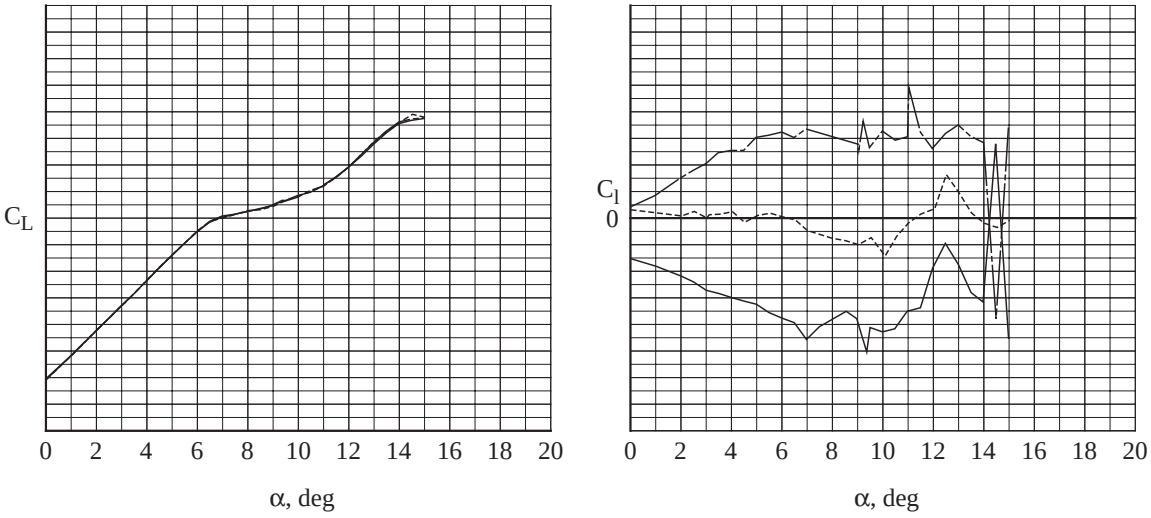

Figure 18. (c) M = 0.8 and LEF/TEF/Ail at 6º/8º/4º.

	Tunnel-Test	Configuration	Run	M_∞	β, deg	Rn, millions/ft	LEF/TEF/Ail
———	16FTT-523	F/A-18E/F: Baseline	164.	0.7997	1.994	3.681	10°/10°/5°
---------	16FTT-523	F/A-18E/F: Baseline	163.	0.7997	-0.1275	3.721	10°/10°/5°
———––	16FTT-523	F/A-18E/F: Baseline	165.	0.8000	-1.995	3.676	10°/10°/5°

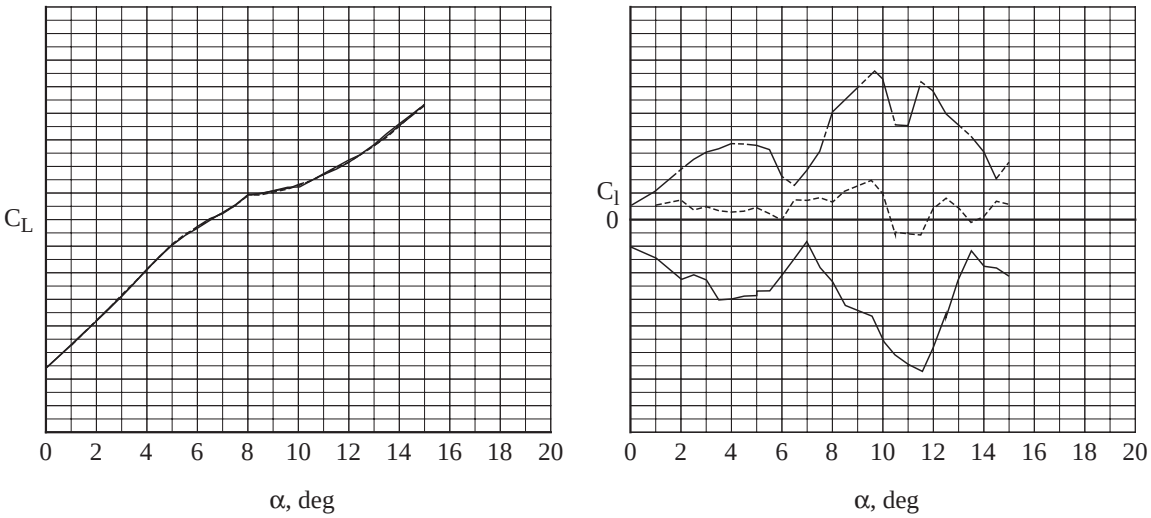

Figure 18. (d) M = 0.8 and LEF/TEF/Ail and 10º/10º/5º.

Discussion of β Effects

Firstly, there is no noticeable effect on the C_L vs. α curve with β for all the test conditions noted in Figure 18. This would be expected for these small β values. Secondly, the C_l vs. α curve at $\beta = 0^o$ is not constant, as has been seen previously in Figures 6(a) and 7(a). (Note that all the C_l vs. α curves in Figure 18 have the same vertical scale, but it is smaller than previously used.) Thirdly, there is ≈symmetry of the C_l curve at $\beta = \pm 2^o$ about that at $\beta = 0^o$. Fourthly, there is a reduction in the C_l growth with increasing α for $\beta = \pm 2^o$ due to the windward wing stalling first. Depending on the flap set and Mach number, the consequence of this growth reduction may be a problem. When this reduction leads to a "necking down" of these curves or for a sign change in the curves (a reversal) — as seen for the $10^o/10^o/5^o$ flap set at M = 0.9, the resulting $C_{l\beta}$ term for the airplane model goes from << 0 for $\alpha \leq 5^o$, towards < 0 for $5^o < \alpha < 6.5^o$, and even to > 0 at $\alpha = 7^o$. A similar cycle is repeated starting at $\alpha = 8^o$. Remember that the $C_{l\beta}$ is a part of the "spring component" and a positive value is not restorative. Lastly, it is interesting to note that many of the breaks in the C_L vs. α curve appear in the vicinity of rapid changes in the C_l vs. α curve. This is to be expected because separation on one wing will undoubtedly impact the overall lift of the wing.

	Tunnel-Test	Configuration	Run	M_∞	β, deg	Rn, millions/ft	LEF/TEF/Ail
———	16FTT-523	F/A-18E/F: Baseline	72	0.8990	-0.1201	3.706	6°/8°/4°
---------	16FTT-523	F/A-18E/F: Baseline	176	0.9000	-0.1196	3.721	10°/10°/5°
———––	16FTT-523	18-inch ISE	257	0.8998	-0.1179	3.915	10°/10°/5°

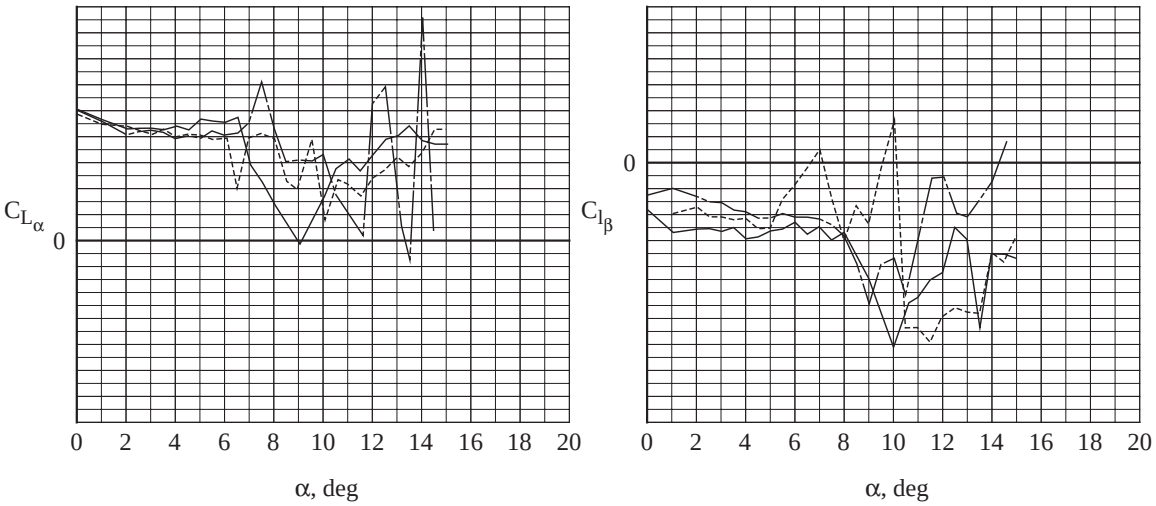

Figure 19. $C_{l\alpha}$ and $C_{l\beta}$ for the pre-production F/A-18E with geometry variations at two Mach numbers. (a) M = 0.9.

	Tunnel-Test	Configuration	Run	M_∞	β, deg	Rn, millions/ft	LEF/TEF/Ail
———	16FTT-523	F/A-18E/F: Baseline	53	0.7987	-0.1286	3.696	6°/8°/4°
---------	16FTT-523	F/A-18E/F: Baseline	163	0.7997	-0.1274	3.722	10°/10°/5°
———––	16FTT-523	18-inch ISE	251	0.7992	-0.1271	3.791	10°/10°/5°

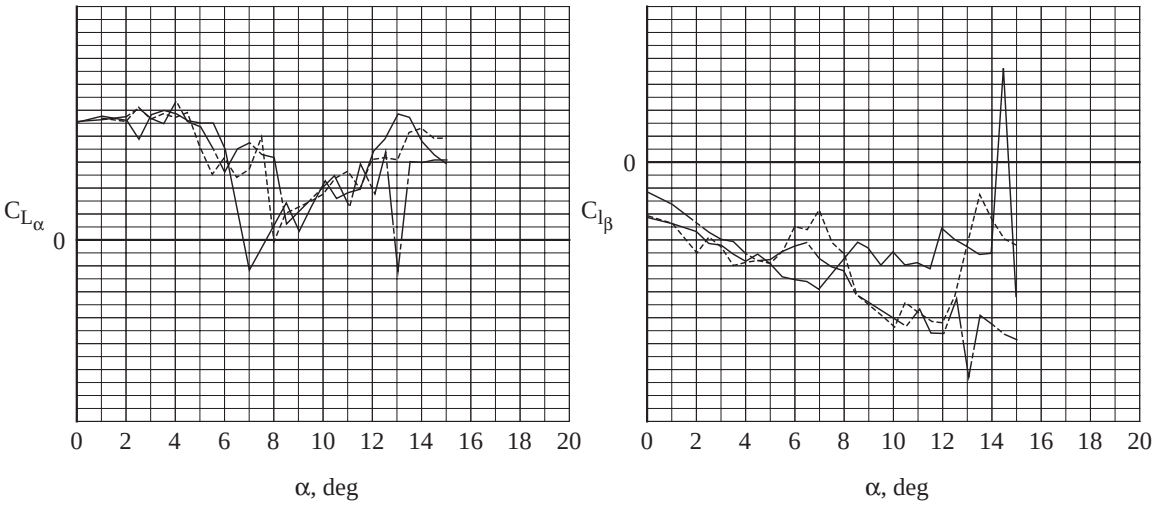

Figure 19. (b) M = 0.8.

Discussion of Derivatives

Figure 19 shows the $C_{L\alpha}$ and the $C_{l\beta}$ terms for the three pre-production F/A-18E configurations studied previously at M = 0.9 and 0.8. They appear together in order to do two assessments. The first is to examine whether any variation in one axis will impact the results of the other (a correlation); i.e., a lift-curve break ($C_{L\alpha}$ change) precedes or follows a reduction in $C_{l\beta}$. The second is to ascertain whether the results sort themselves out in a manner similar to the flight data in terms of delay of AWS onset.

(1) For the correlation study, there is an apparent one noted for the $10^o/10^o/5^o$ flaps, with and without the 18"ISE, in that for sharp reductions in $C_{L\alpha}$ there are sharp increases (less negative values) for $C_{l\beta}$. However, there is no such correlation for the $6^o/8^o/4^o$ flaps at M = 0.9 and none for any flap sets at M = 0.8.

From this limited study, if a correlation exits between the lateral and longitudinal parameters it may only be in some combinational form; such as a product or ratio of the values — actual or absolute — or in the α derivatives of the combinations. Other parameters, such as $C_{l\alpha}$ and C_l, should also be considered in another study.

One difficulty in trying to establish correlation with any of these parameters and the FTR response data is the need to formulate a reasonable and defensible aerodynamic behavior expected for any

such combination during an AWS event. All this is the subject of future work.

(2) Regarding whether these data sort themselves in the manner of flight, there are no trends apparent.

Alternative FOM-Static Ratings

Ratings of these static AFOMs will await the results of additional studies, as the results to date have been inconclusive.

RECOMMENDATIONS

There are four recommendations that can be drawn from a comparison of the static and FTR response data for these four fighter models. First, if possible, employ wing-root-bending-moment gauges for each new model to help distinguish buffet from AWS events. Second, if the model is seen to be dynamically active during its initial testing at transonic speeds, then it is imperative that small α increments be taken in and around the α regions where the activity is noted. Third, examine all the Traditional FOMs closely. In particular, the lift curve slope, the rolling-moment and wing-root-bending-moment static and rms data as they can be meaningful indicators of a possible region of unwanted lateral flight activity. Close attention should be paid to those α ranges where there is a rapid change or excursion of a TFOM. However, since the TFOMs can give false positives with respect to AWS events, use the FTR rig.

CONCLUDING REMARKS

This paper has examined Traditional and Alternate Figures Of Merit (FOMs) — TFOMs and AFOMs — for four current fighter aircraft models. The data used in these FOMs was obtained from static testing of these models at transonic and subsonic speeds. There are two main themes in this paper. The first is whether there is a static FOM that is both a necessary and sufficient condition for predicting an Abrupt Wing Stall (AWS) event as indicated by Free-To-Roll (FTR) response data. The result for both the TFOMs and AFOMs is NO, not with 100% certainty. In particular, the TFOMs indicate merely necessary conditions but they are not always sufficient and the AFOMs are still in the development stage. Some of the TFOMs, namely, the lift-curve slope and the rolling-moment and wing-root-bending-moment static and rms data, indicated potential AWS events for certain combinations of configurations and Mach numbers, but not all which had events. The TFOMs can give false positives.

The second theme is whether an examination of the TFOMs alone would sort the four models in groups of those likely to have AWS events and those unlikely. The result is that all four models would be expected to have some AWS events based on the stringent criteria established. So the TFOMs did not sort out the chosen models from an AWS event perspective. This is of special importance when one remembers that the data processed did not take into account the flap schedule.

A corollary to the second theme is whether the static Figures Of Merit or

the FTR-FOM would show significant differences, in general, between the two configurations that exhibit wing drop and the two that did not. As seen in the summary tables, there were not clear differences between the two wing droppers – pre-production F/A-18E and the AV-8B at the extremes of its flight envelope – and the F/A-18C. This lack of distinction is not the result of any shortcomings in the Figures Of Merit. Instead, the lack of distinction was due to the fact that the F/A-18C would have been a very active dropper if its flap schedule had been different. That is, the lateral activity for the F/A-18C seen in the wind tunnel was at angles of attack higher than the angle of attack at which the aircraft flies for the given flap settings. This just underscores that a properly conceived flap schedule can avoid many flight handling-qualities problems, like wing drop, which might otherwise occur. However, simply modifying flap schedule alone is not always sufficient to resolve these uncommanded motions, as was determined for the pre-production F/A-18E.

Other Remarks:

From the wind-tunnel study in which the pre-production F/A-18E had two different flap schedules simulated, as well as an 18" inboard snag, the resulting AFOMs-Unsteady predicted the same α ordering for AWS improvement as had been noted in flight.

SUMMARY

This paper documents the development of various potential Figures Of Merit (FOMs) from static wind-tunnel tests and the extent to which they have proven useful in the prediction of Abrupt Wing Stall (AWS) events at high-subsonic and transonic speeds on four fighter aircraft models. These models are, namely; the pre-production version of the F/A-18E that experienced wing drop and which was later modified to correct the problem, the AV-8B at extremes of its flight envelope, the F/A-18C and the F-16C. From flight tests, it is known that the first two configurations can experience wing drop while the last two do not. The FOMs considered range from: (1) basic static-data and slopes; (2) combinations of (1); (3) rms values of selected force/moment components; (4) combinations of (3); and (5) rms and static values of wing-root-bending moments, where available. No one parameter works for all configurations but some are better indicators than others when compared to the Free-To-Roll (FTR) response data.

The conclusion from this study is that the Traditional FOMs (TFOMs), obtained in a static wind-tunnel test, can by themselves give some indication as to whether a new aircraft configuration will experience AWS events in flight. However, they may yield as many or more false positive flags than are recorded by the FTR response data. Since the FTR response data compare favorable with flight data, it is taken as the standard. This means that for full certainty regarding AWS events on a new airplane, one needs the FTR response data as the TFOMs were determined to be necessary but not sufficient conditions.

The results of an Alternate FOMs study determined that the studied parameters

were also not able to reliably predict FTR response data for all four models.

REFERENCES

1. Chambers, Joseph R.; and Hall, Robert M.: *Historical Review of Uncommanded Lateral- Directional Motions at Transonic Conditions (Invited)*. AIAA Paper 2003-0590, presented at the 41st AIAA Aerospace Sciences Meeting and Exhibition in Reno NV, Jan. 6-9, 2003.

2. *The Effects of Buffeting and other Transonic Phenomena on Maneuvering Combat Aircraft.* AGARD-AR-82, Sect. 1.5.3, July 1975.

3. *Manoeuvre Limitations of Combat Aircraft*. AGARD-AR-155A, August 1979.

4. Capone, F.J.; Owens, D.B.; and Hall, R.M.: *Development of a Free- To- Roll Transonic Test Capability.* AIAA Paper 2003-0749, presented at the 41st AIAA Aerospace Sciences Meeting and Exhibition in Reno NV, Jan. 6-9, 2003.

5. McMillin, S.N.; Hall, R.M.; and Lamar, J.E.: *Transonic Experimental Observations of Abrupt Wing Stall On an F/A-18E Model.* AIAA Paper 2003-0591, presented at the 41st AIAA Aerospace Sciences Meeting and Exhibition in Reno NV, Jan. 6-9, 2003.

6. Schuster, D.M.; and Byrd, J.E.: *Transonic Unsteady Aerodynamics of the F/A-18E at Conditions Promoting Abrupt Wing Stall*. AIAA Paper 2003-0593, presented at the 41st AIAA Aerospace Sciences Meeting and Exhibition in Reno NV, Jan. 6-9, 2003.

7. Kashafutdinov, Dr. Stanislav: Private communication to Robert M. Hall, 1998.

8. Ross, A. Jean: *Flying Aeroplanes in Buffet.* Aeronautical Journal, October 1977, pp. 427-436.

9. Bore, Cliff L.: *Post-Stall Aerodynamics of the "Harrier" GR1*. In AGARD-CP-102 Fluid Dynamics of Aircraft Stalling, November 1972.

10. Owens, D.B; Brandon, J.; Capone, F.J.; Hall, R.M.; and Cunningham, K.: *Free- To- Roll Analysis of Abrupt Wing Stall on Military Aircraft at Transonic Speeds.* AIAA Paper 2003-0750, presented at the 41st AIAA Aerospace Sciences Meeting and Exhibition in Reno NV, Jan. 6-9, 2003.

11. Capone, F.J.; Hall, R.M.; Owens, D.B.; Lamar, J.E.: and McMillin, S.N.: *Recommended Experimental Procedures for Evaluation of Abrupt Wing Stall Characteristics.* AIAA Paper 2003-0922, presented at the 41st AIAA Aerospace Sciences Meeting and Exhibition in Reno NV, Jan. 6-9, 2003.

12. Gainer, Thomas G.; and Hoffman, Sherwood: *Summary of Transformation Equations and Equations of Motion Used in Free-Flight and Wind-Tunnel Data Reduction and Analysis*. NASA SP-3070, 1972.

13. Kokolios, A.; and Cook, S.: *Use of Piloted Simulation for Evaluation of Abrupt Wing Stall Characteristics (Invited)*. AIAA Paper 2003-0924, presented at the 41st AIAA Aerospace Sciences Meeting and Exhibition in Reno NV, Jan. 6-9, 2003.